the plant journal

SEB SOCIETY FOR EXPERIMENTAL BIOLOGY

The Plant Journal (2026) **126,** e70833 doi: 10.1111/tpj.70833

TECHNICAL ADVANCE

Artificial soil (ArtSoil): Recreating soil conditions in synthetic plant growth media

Vera Kaplunova[1,†], Houda Alioui[1,†], Tobias Griguschies[1], Luca Müller[1], Vivien Joisten-Rosenthal[2], Tobias Lautwein[3], Sabine Metzger[4,5], Paloma Durán[6] and Eliza Loo[1,4,*]

[1]*Faculty of Mathematics and Natural Sciences, Institute for Molecular Physiology, Heinrich Heine University Düsseldorf, Düsseldorf, Germany,*

[2]*Faculty of Mathematics and Natural Sciences, Institute for Biological Data Science, Heinrich Heine University Düsseldorf, Düsseldorf, Germany,*

[3]*Biologisch-Medizinisches Forschungszentrum, Genomics & Transcriptomics Labor, Heinrich Heine University Düsseldorf, Düsseldorf, Germany,*

[4]*Cluster of Excellence on Plant Sciences, Düsseldorf, Germany,*

[5]*Institute for Plant Sciences, Cluster of Excellence on Plant Sciences (CEPLAS), Cologne Biocenter, University of Cologne, Cologne, Germany, and*

[6]*LIPME, INRAE, CNRS, Université de Toulouse, 31326 Castanet-Tolosan, France*

Received 9 October 2025; revised 13 February 2026; accepted 11 March 2026.
*For correspondence (e-mail loo@hhu.de).
†These authors contributed equally to this work.

SUMMARY

Controlled plant growth in laboratories can be achieved by cultivating plants under sterile or axenic conditions on predefined synthetic growth media, typically supplemented with sugar. In nature, plants do not receive exogenous sugar supplies, form symbiosis with microbes, and plant growth is influenced by soil edaphic factors. Thus, physiological and multi-omic analyses of plants grown on synthetic media will differ from those of soil-grown plants due to the influence of sucrose, and the absence of microbiota and soil edaphic factors on plant growth. The rapid advances in spatial omics call for accurate characterization of plants grown under conditions similar to soil. To address the issue, we developed Artificial Soil (ArtSoil), a growth medium containing essential nutrients for plant growth, and aqueous soil extract (ASE) to maintain soil microbiomes and edaphic factors, simultaneously eliminating the need for sugar supplementation in the medium. We compared *Arabidopsis thaliana* grown on conventional media and on ArtSoil under various growth conditions. We showed that complex soil microbiota in ArtSoil promote plant growth without physiological side effects induced by sucrose. We demonstrate an application for ArtSoil in single-cell transcriptomics and report microbiota-induced cell-type-specificity in immune and nitrogen signaling. We tested ArtSoil with six types of ASEs to demonstrate its potential to decouple nutrient effects from microbiota in plant growth. We conclude that ArtSoil offers a more physiologically relevant alternative to conventional media for studying plant growth within a soil-like context.

Keywords: technical advance, axenic growth, microbiome, root, single-cell, soil-based growth media, sucrose, synthetic ecosystem.

INTRODUCTION

A basic requirement in plant research is a gold standard for plant growth conditions, that is, reproducible conditions as similar as possible to natural growth. Temperature, humidity, light intensity, and diurnal cycle are usually standardized. Since the soil environment is highly heterogeneous, it is common practice to use synthetic growth media to study the effects of specific parameters on the growth and development of mutant and wild-type plants. Various culture media with defined concentrations of macro- and microelements, pH, and gelling agents have been formulated (Gamborg et al., 1968; Hoagland & Armon, 1950; Murashige &

Skoog, 1962; Schenk & Hildebrandt, 1972). In most cases, growth media are supplemented with sucrose and are kept sterile. It is intriguing that despite the natural ability of plants to photosynthesize to produce sugars, effective axenic growth requires supplementation of the synthetic media with glucose or sucrose. In natural conditions, plants require their microbiome for normal growth and to thrive under stress (Berendsen et al., 2018; Carrión et al., 2019; Castrillo et al., 2017; Durán et al., 2018; Kwak et al., 2018). By contrast, *in vitro* growth is typically conducted in microbe-free conditions.

Sucrose or glucose supplementation in growth media is essential for efficient *Arabidopsis thaliana* (*A. thaliana*) growth as sucrose stimulates root and shoot growth. Sucrose supplementation is also required for *A. thaliana* seed filling and proper embryo formation (Chen et al., 2015; Miotto et al., 2021; Roycewicz & Malamy, 2012). Despite the widespread use of sucrose in plant cultivation media, sucrose toxicity can inhibit radicle and primary root growth (Liu, Long, et al., 2022) as well as seed germination (Li et al., 2012; Yang et al., 2004). Sucrose supplementation also alters nitrogen and carbohydrate metabolism (Huang et al., 2022; McLaughlin et al., 2023; Tan et al., 2022). Growing *A. thaliana* seedlings on sucrose-supplemented media could mask the growth phenotypes of certain mutants (Chen et al., 2015; Fan et al., 2025). For instance, the sucrose uniporter *sweet11;12* double mutants exhibit root growth retardation when grown on sucrose-free media, a phenotype that is masked or compensated for when the seedlings are grown on sucrose-supplemented media (Chen et al., 2015). Sucrose affects *A. thaliana* throughout the plant's developmental stages as evidenced by contrasting patterns of defense-related genes induction in 9 versus 14-day-old seedlings (Siffert & Sasse, 2024). The use of sucrose in growth media, thus, poses a complex uncoupling of authentic plant responses from sucrose-induced responses.

Besides altering root hair growth (Claeijs & Vissenberg, 2022), single-cell analyses revealed that roots of sterile *A. thaliana* seedlings grown on sucrose-supplemented media have higher proportions of developmentally mature cells and altered expression of genes that are highly specific to distinct cell populations (Shulse et al., 2019). Root development studies are limited by ecological accuracy since potential mechanisms of root responses mediated by the soil- and root-associated microbiota are not captured in standard growth media (Dini-Andreote et al., 2025). Due to the importance of microbiota for plant growth and development (Durán et al., 2018; Garrido-Oter et al., 2018), synthetic microbial communities and gnotobiotic plant growth systems have been established (Bodenhausen et al., 2014; Gao et al., 2018; Kremer et al., 2021; Ma et al., 2022). The important discoveries have facilitated our understanding of microbiota function, but it remains crucial to study the role of microbiota and plant under ecosystem-relevant conditions where the total soil microbial community and soil edaphic factors can be captured (Chesneau et al., 2025). Synthetic growth media affect bacterial fitness for colonizing host plants (Torres et al., 2025). Soil properties including nutrients and pH directly affect soil microbial community structure and consequently, microbiota assembly (Bakker et al., 2018). Although individual strains and consortia of plant-beneficial microbes have been identified (Daniel et al., 2022; de Souza et al., 2015; Gouda et al., 2018; Poria et al., 2022), a major challenge in translating microbiota research to the field is integrating the beneficial strain or consortia with the native microbiota (Liu et al., 2024; Russ et al., 2023; Sessitsch et al., 2019). Gnotobiotic systems often cannot fully capture the diversity and complexity of soil microbial communities, which may lead to overlooking important factors that affect community assembly, for example, priority effects (Carlström et al., 2019; Fukami, 2015; Wippel et al., 2021) and regionalization of microbiota colonization along the root (Loo et al., 2024).

Extensive efforts to inform the scientific community about synthetic community design exemplify the complexity of synthetic community design (Durán et al., 2025; Mehlferber et al., 2024; Northen et al., 2024). One approach to addressing the challenges posed by sterile sucrose-supplemented media and the complexity of synthetic communities is to use a sucrose-free medium containing self-equilibrating, complex soil microbial communities. Here, we present Artificial Soil (ArtSoil), which enables plant cultivation under soil-nurturing growth conditions while enabling controlled environmental conditions and full access to the roots. ArtSoil is a synthetic growth medium supplemented with an aqueous soil extract (ASE) containing soil microbiota to support growth, hence eliminating the need for sucrose supplementation in the medium (Figure 1). We optimized and compared plants grown on ArtSoil with synthetic growth media supplemented with or without sucrose under various growth conditions and showed that ArtSoil supported plant growth with higher shoot biomass and complex root architecture and without negative side effects introduced by sucrose. We demonstrate an application of ArtSoil in single-cell transcriptomics of *A. thaliana* roots and report cell-type-specificity in root microbiota-induction of defense and nitrogen signaling, as well as possible sucrose-induced artifacts in plant–microbe studies. We challenged ArtSoil with six different ASEs and demonstrated the potential to separate nutrient effects from microbiota promotion of plant growth.

RESULTS

Effects of microbial load on root microbiota diversity and plant growth on ArtSoil

The ASE provides soil microbial communities to the growth media. Since microbial load and diversity affect the community stability (Cook et al., 2006; Van Elsas

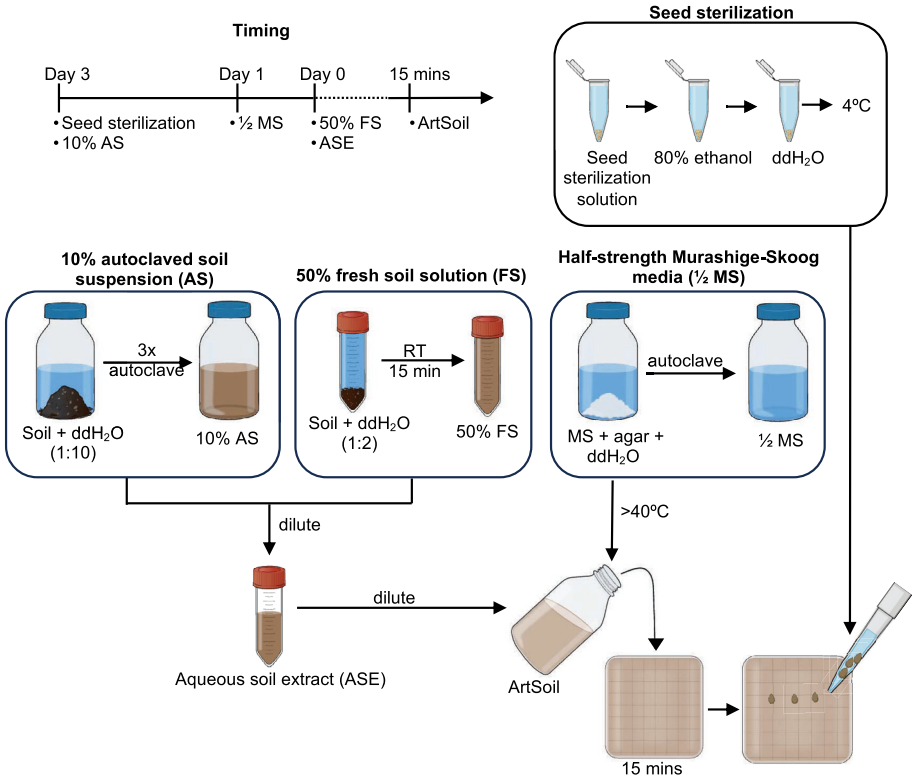

Figure 1. Preparation of ArtSoil.
Overview of the steps involved in the preparation of ArtSoil. ArtSoil is composed of three main components, that is, 10% autoclaved soil solution (10% AS), 50% fresh soil solution (50% FS), and ½ MS without sucrose supplementation. Three days before the assembly of ArtSoil, seeds should be sterilized and 10% AS should be prepared for three consecutive autoclaves. One day before the assembly of ArtSoil plates, ½ MS without sucrose supplementation should be prepared for autoclave. On the day of plate assembly, 50% FS should be prepared and diluted accordingly with 10% AS to produce ASE. The ASE will be added into ½ MS without sucrose supplementation to produce ArtSoil. ArtSoil can be subsequently poured into open or closed Petri dishes and left to cool for the agar to solidify before sowing seeds.

et al., 2012; Wippel et al., 2021), it is crucial to determine the optimal dilution of ASE, hence, the amount of microbes used for establishing the microbial community in ArtSoil. The dilution-to-extinction approach was adopted to determine the optimal microbial load for establishing a stable *in situ* community (Cook et al., 2006; Korenblum et al., 2020; Van Elsas et al., 2012). To demonstrate the effects of ASE dilution on plant growth, three dilutions, that is, 10^{-2}, 10^{-4}, and 10^{-6} of the Cologne Agricultural Soil (CAS) extract were used for establishing the microbial community in ArtSoil (Method S1). The Shannon-Weaver diversity index was used to measure microbial diversity. The index typically ranges from 1.5 to 3.5 and rarely exceeds 4.5 (Ortiz-Burgos, 2016). CAS had a microbial Shannon-Weaver diversity of 4.3, while roots of CAS-grown *A. thaliana* have a Shannon-Weaver diversity index of 3.4 (Figure 2a). Bulk media from ArtSoil^{CAS} (agar from ArtSoil plates without plants) with 10^{-2}, 10^{-4}, and 10^{-6} dilutions of CAS had Shannon-Weaver diversity indices of 3.6, 3.0, and 3.0, respectively, indicating reduced microbial diversity in ArtSoil^{CAS} compared to CAS but within the range of expected diversity index. The Shannon-Weaver diversity index of microbes derived from roots of plants grown on ArtSoil^{CAS} inoculated with 10^{-2}, 10^{-4}, and 10^{-6} of CAS were 2.9, 2.6, and 3.4, respectively. The diversity of microbes from the roots of *A. thaliana* grown on ArtSoil^{CAS} with 10^{-6} dilution of CAS (Shannon-Weaver index 3.4) most closely resembled the diversity of microbes derived from plants grown on soil (Shannon-Weaver index 3.4). The community structures of root-associated microbiota derived from ArtSoil reconstituted the core root microbiota (Bulgarelli et al., 2013; Lundberg et al., 2012) with 10^{-4} dilution of CAS most closely resembling CAS-grown *A. thaliana* (Bulgarelli et al., 2012; Schlaeppi et al., 2014) (Figure 2b).

It should be noted that an imbalance in bacterial abundance may result in plant susceptibility to opportunistic pathogens indicated by reduced plant growth (Ma et al., 2021). Roots of plants from ArtSoil^{CAS} inoculated with 10^{-2} dilution of CAS have a higher Shannon-Weaver diversity index compared to roots from ArtSoil with 10^{-4} dilution of CAS. However, plants grown on ArtSoil^{CAS}

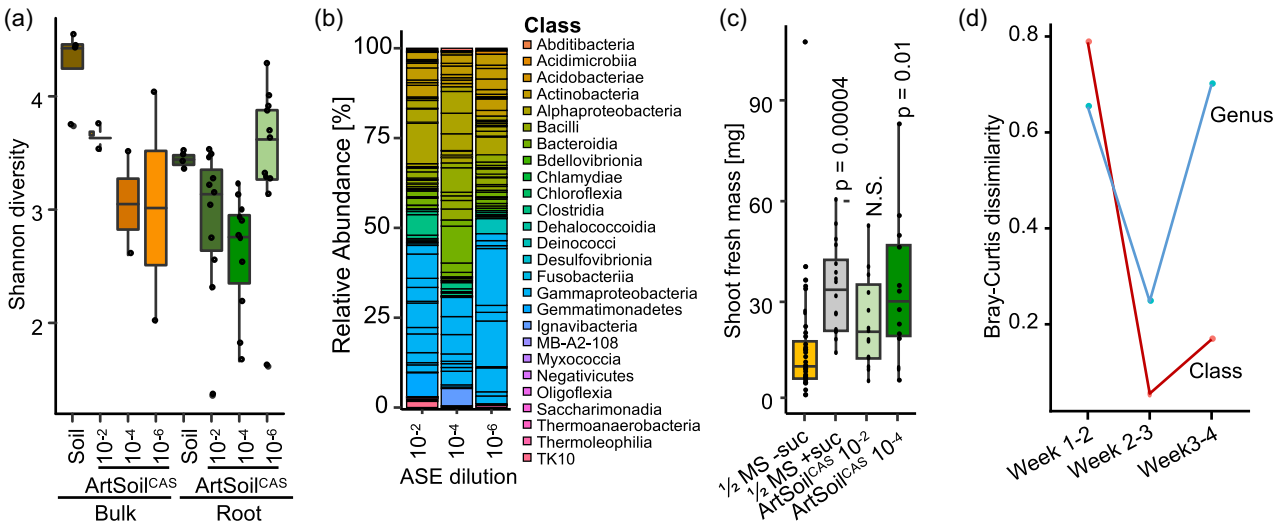

Figure 2. Dilution of ASE influences plant growth on ArtSoil.
(a) The Shannon-Weaver diversity of root microbiota from 4-week-old *A. thaliana* plants grown on ArtSoil with 10^{-2}, 10^{-4}, or 10^{-6} dilutions of ASE in a closed system. "Bulk" indicates microbial community derived from soil or ArtSoil media without plants. "Root" indicates microbial community derived from roots of plants grown on soil or ArtSoil with indicated dilutions of ASE. Microbiota profiling performed via 16S amplicon sequencing, $N > 9$.
(b) Relative abundance of root microbiota derived from 4-week-old *A. thaliana* plants grown on ArtSoil with 10^{-2}, 10^{-4}, or 10^{-6} of ASE. Colors correspond to taxonomy at the class level listed in the legend. Each bar represents normalized relative abundance from $N > 5$.
(c) Shoot fresh mass of *A. thaliana* seedlings from grown on ArtSoil with 10^{-2} or 10^{-4} dilution of ASE compared to sterile ½ MS media ± suc. All assays were repeated three times using independent ASE batches to ensure data reproducibility, $N > 15$. *P* values were calculated via Student's *t*-test against ½ MS media without sucrose supplementation (½ MS –suc). N.S., not significant. The top and bottom boundaries of each boxplot indicate the first and third quartiles, the center line indicates the median, and the whiskers represent 1.5× the interquartile range from the first and third quartiles.
(d) Microbial turnover in ArtSoilCAS. Bray–Curtis analysis performed using full-length 16S amplicon sequencing of bulk ArtSoilCAS over 4 weeks.

inoculated with 10^{-2} dilution of CAS lacked growth promotion conferred by the microbiota compared to sterile ½ MS without sucrose (Figure 2c), indicating possible microbial overload. Since ASEs vary in microbial loads and diversity, users are advised to test a series of dilutions to determine the optimal ASE dilution for ArtSoil. Since ArtSoil^{CAS} with a 10^{-4} dilution of ASE was able to reconstitute the root microbiome without plant growth penalty (Figure 2c), subsequent analyses were performed on plants grown on ArtSoil^{CAS} with 10^{-4} dilution of ASE.

To ensure that the microbial load in ArtSoil^{CAS} is consistent, colony-forming units (CFU) for independent preparations of ArtSoil^{CAS} with 10^{-4} dilution were calculated. The mean CFU/mL values ranged from 5.2 to 8.8 × 10^6 (Figure S1A). CFU/mL measurements were of the same order of magnitude, indicating reproducible microbial load across independent ArtSoil preparations. Since ArtSoil was developed based on microbial self-repopulation, 16S amplicon counts were used as a proxy for microbial abundance. The total number of full-length amplicon sequences obtained increased from week 1 (1.2 million reads) to week 2 (2.4 million reads), after which saturation was achieved (Figure S1A). To determine whether population saturation indicated community stability, community turnover over 4 weeks was examined. At a higher taxonomic level (class), the relative abundance stabilized after 2 weeks of ArtSoil^{CAS} cultivation without plants (Figure S1B). At the lower taxonomic level (genus), the number of unique genera gained and lost in ArtSoil^{CAS} was more dynamic, averaging 41 genera gained and 48 genera lost per week. Accordingly, Bray–Curtis dissimilarity index indicated a decrease in beta-diversity at the class level but a sharp increase at the genus level over the span of 4 weeks (Figure 2d). Collectively, data suggest that bacterial community turnover in ArtSoil was driven by shifts at the genus level rather than in the dominant class.

Influence of ArtSoil on plant development in different growth systems

Plant growth in the closed systems (i.e., sealed Petri dishes) typically causes the accumulation of ethylene and carbon dioxide gases, decreases transpiration due to increased humidity and limited air circulation, reduces cuticle formation, and experiences different utilization of red to far-red light ratio due to wavelengths absorbed by the plastic (Nagel et al., 2020). Consequently, cultivation in a closed system penalizes shoot and root development. ArtSoil alleviates physiological stress in plants grown in a closed system, as evidenced by increased shoot biomass and root length (Figure 3a). Petioles of *A. thaliana* grown on half-strength Murashige–Skoog (½ MS) without sucrose supplementation (MS –suc) in a closed system were elongated, whereas plants grown on closed system ArtSoil^{CAS} are visibly larger and have extensive root growth and

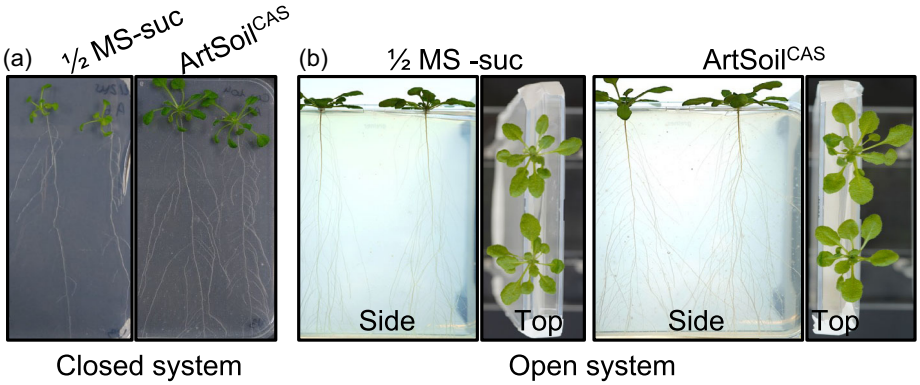

Figure 3. *A. thaliana* growth on ArtSoil in a closed or open system.
(a) Comparison of phenotypes of 4-week-old *A. thaliana* grown on ½ MS without sucrose supplementation, and ArtSoil with CAS as ASE (ArtSoilCAS) in a closed system where shoots and roots were enclosed in sealed Petri dishes.
(b) Side and top view of 4-week-old *A. thaliana* plants grown on ½ MS without sucrose supplementation, or on ArtSoilCAS in an open system where shoots are exposed to air and roots were enclosed in Petri dishes wrapped with aluminum foil (in darkness).

branching (Figure 3a). To test whether ArtSoil could support plant growth beyond physiological stresses introduced in confined growth chambers, ArtSoil was applied to an open plant growth system (Nagel et al., 2020). Compared to the closed system, 4-week-old *A. thaliana* grown on MS –suc in the open system had larger rosette diameters without petiole elongation and a substantially higher root mass (Figure 3b). Plants grown on ArtSoil^{CAS} in an open system had higher shoot biomass and root branching density compared to plants grown on MS –suc (Figure 3b). Thus, ArtSoil^{CAS} promotion of plant growth extends beyond alleviating physiological stresses in closed growth systems.

ArtSoil does not introduce sucrose-induced artifacts on plant growth

Under sterile growth conditions, sucrose supplementation in growth media promotes *A. thaliana* growth (Kircher & Schopfer, 2023; Pereyra et al., 2022; Roycewicz & Malamy, 2012). Evidently, the shoot fresh mass of 4-week-old *A. thaliana* grown under optimal light intensity (120 μmol m^{-2} s^{-1}) on MS –suc was significantly lower compared to seedlings grown on MS + suc (Figure 4a). The shoot fresh mass of seedlings grown on ArtSoil^{CAS} was significantly higher compared to seedlings grown on MS –suc, but not significantly different compared to seedlings grown on MS + suc. Under suboptimal light intensity, microbiota alleviates plant growth retardation (Hou et al., 2021). Accordingly, the shoot fresh mass of plants grown under low light intensity (25 μmol m^{-2} s^{-1}) on ArtSoil^{CAS} was significantly higher than plants grown on MS –suc (Figure 4a). Under low-light conditions, exogenous sucrose application can promote root development (Miotto et al., 2021; van Gelderen et al., 2018). The roots of *A. thaliana* seedlings grown at low light intensity (25 μmol m^{-2} s^{-1}) on MS –suc or ArtSoil^{CAS} were significantly shorter compared to seedlings grown on MS + suc (Figure 4b; Figure S2), indicating that ArtSoil^{CAS} does not artificially induce root growth under suboptimal light conditions. Under optimal light intensity (120 μmol m^{-2} s^{-1}), roots of 1–3-week-old seedlings grown on MS –suc or on ArtSoil^{CAS} were significantly shorter compared to roots from seedlings grown on MS + suc (Figure S2). Notably, roots of 4-week-old seedlings grown on ArtSoil^{CAS} were not significantly different in length compared to roots of seedlings grown on MS + suc (Figure 4b, Figure S2). Root growth promotion was pronounced after 4 weeks of growth on ArtSoil^{CAS}, a duration that coincides with the duration required for microbial colonization of the root to stabilize (Edwards et al., 2015; Zhou et al., 2024).

Although sucrose is beneficial for *in vitro* plant growth, sucrose can also reduce seed germination efficiency (Li et al., 2012). Here, only 35% of *A. thaliana* seeds sown on MS + suc exhibited cotyledon emergence 2 days after sowing compared to 74% of seeds with cotyledon emergence when sown on MS –suc (Figure 4c). Similar to MS –suc, cotyledons emerged from 83% of seeds 2 days after sowing on ArtSoil^{CAS} (Figure 4c). Collectively, our data indicated that ArtSoil enables the cultivation of *A. thaliana* without the need for sugar supplementation, thereby eliminating potential unphysiological effects of sucrose on plant growth.

Single-cell analysis of ArtSoil-grown roots reveals cell-type-specific transcriptomic changes induced by microbiota

To investigate whether ArtSoil eliminates sucrose-induced artifacts at the cellular level, two independent replicates of single-cell transcriptomics were performed on 7-day-old *A. thaliana* roots grown on ArtSoil^{CAS}. A total of 14 100 cells (8000 and 6100 cells) were sequenced, producing a mean

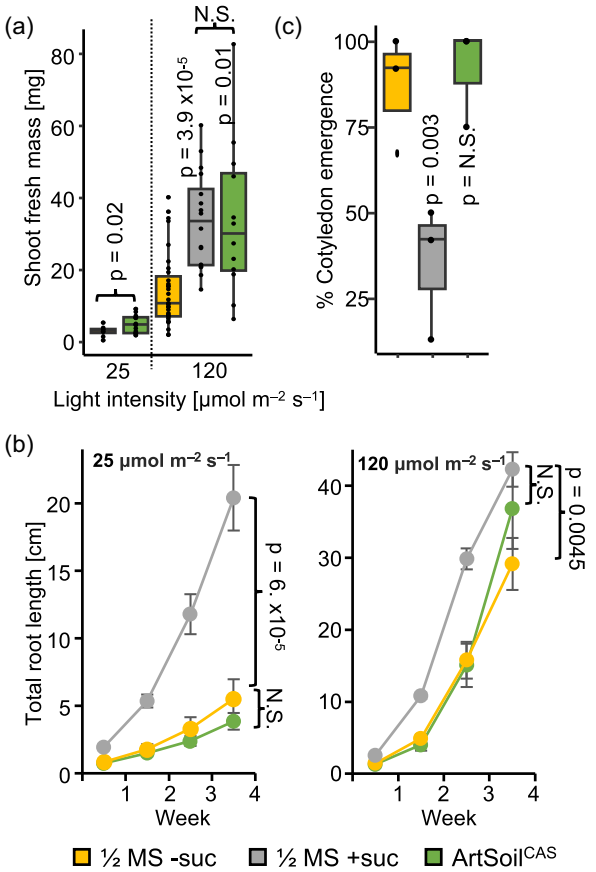

Figure 4. ArtSoil supports *A. thaliana* growth without side effects from sucrose supplementation in synthetic growth media.
(a) Shoot fresh mass of 4-week-old *A. thaliana* grown on sterile media or in a closed system on ArtSoilCAS under suboptimal (25 µmol m^{-2} s^{-1}) or optimal (120 µmol m^{-2} s^{-1}) light conditions.
(b) Total root length of *A. thaliana* grown on sterile media or in a closed system on ArtSoilCAS for 1 to 4 weeks under suboptimal (25 µmol m^{-2} s^{-1}) or optimal (120 µmol m^{-2} s^{-1}) light conditions. Error bars indicate standard errors.
(c) Percentage cotyledon emergence of *A. thaliana* sown on sterile media or in a closed system on ArtSoilCAS 2 days after sowing. All assays were repeated three times, using independent ASE batches to ensure data reproducibility, $N > 15$. *P* values were calculated via Student's *t*-test against ½ MS without sucrose supplementation (½ MS –suc). N.S., not significant. The top and bottom boundaries of each boxplot indicate the first and third quartiles, the center line indicates the median, and the whiskers represent 1.5× the interquartile range from the first and third quartiles.

of 23 122 reads per cell, and a median of 2302 genes per cell. To quantify the reproducibility of the two independent datasets, three proxies were computed: (i) Jaccard similarity to quantify transcriptome overlap, (ii) transcriptomic profiles correlation, and (iii) cell-type correlation. All measured proxies exceeded the threshold of 0.9 (Jaccard: 0.93, transcriptome correlation: 0.93, cell-type correlation: 0.96; Figure S3A), indicating highly overlapping genes with highly correlated expression profiles were found in similar cell types from both replicates. Thus, two independent single-cell transcriptomics studies indicated that *A. thaliana* grown on ArtSoil were reproducible at the cellular level. The two replicates were integrated for subsequent analyses.

UMAP clustering and annotation based on previously established marker genes (https://rootcellatlas.org/) revealed 20 transcriptionally distinct clusters representing the major cell types (Figure 5a). The epidermal cell lineage comprises six clusters, representing 49.7% of the total cell population, including trichoblast and atrichoblast cells from all developmental zones. The ground tissue lineage (18.2%) contained three clusters associated with cortex and/or endodermis cells from the transition (TZ), elongation (EZ), and differentiation zones (DZ). The stele lineage (19.8%) comprised the procambium, xylem pole parenchyma (XPP), phloem companion cells (PCC), and protoxylem, whereas the root cap lineage (11%) comprised the detached cells, lateral root cap, columella, and quiescence center (QC). The transitions between clusters indicated that the UMAP captured the gradual changes in gene expression consistent with the developmental and spatial continuity of the root. Of note, cluster 17 comprises cells whose genes are induced by protoplasts and is therefore excluded from subsequent analyses.

Single-cell transcriptomics of roots from ArtSoil ($Root^{ArtSoil}$) was compared to published single-cell transcriptomics of roots of seedlings grown on sterile media supplemented with 1% sucrose ($Root^{Suc}$) (Shahan et al., 2022). To evaluate the extent to which microbial colonization influences mRNA accumulation in a cell-type-specific manner, the number of differentially regulated genes (DEGs) within each cluster was quantified across both datasets (Figure 5b). Cell clusters in $Root^{Suc}$ were annotated using $Root^{ArtSoil}$ as a reference map to enable direct cell-type-specific comparisons. Clusters 6 and 16 were excluded due to insufficient cell numbers. To assess the potential differential impact of sucrose and microbial presence across radial layer and longitudinal zones of the root, the proportion of genes differentially regulated within each tissue lineage was quantified. Across radial layers, $Root^{ArtSoil}$ showed a significantly greater proportion of DEGs in the stele tissue lineage (52.5% DEGs in $Root^{ArtSoil}$ vs 26.2% in $Root^{Suc}$, Figure S3B). Compared to $Root^{Suc}$, the proportion of DEGs in the root cap lineage was similar in $Root^{ArtSoil}$ (18.9% DEGs in $Root^{ArtSoil}$ vs 18.3% in $Root^{Suc}$), while the epidermal (15.7% DEGs in $Root^{ArtSoil}$ vs 28.8% in $Root^{Suc}$) and ground tissue (12.9% DEGs in $Root^{ArtSoil}$ vs 26.8% in $Root^{Suc}$) lineages exhibited significantly lower proportions. Along the longitudinal axis, the proportion of DEGs in the elongation zone was higher in $Root^{ArtSoil}$ than in $Root^{Suc}$ (58.1% DEGs in $Root^{ArtSoil}$ vs 49.1% in $Root^{Suc}$). In contrast, the differentiation zone showed a higher proportion of DEGs in $Root^{Suc}$, consistent with previous report (Shulse et al., 2019). Thus, pseudobulk DEG analysis indicated that although both sucrose supplementation and the

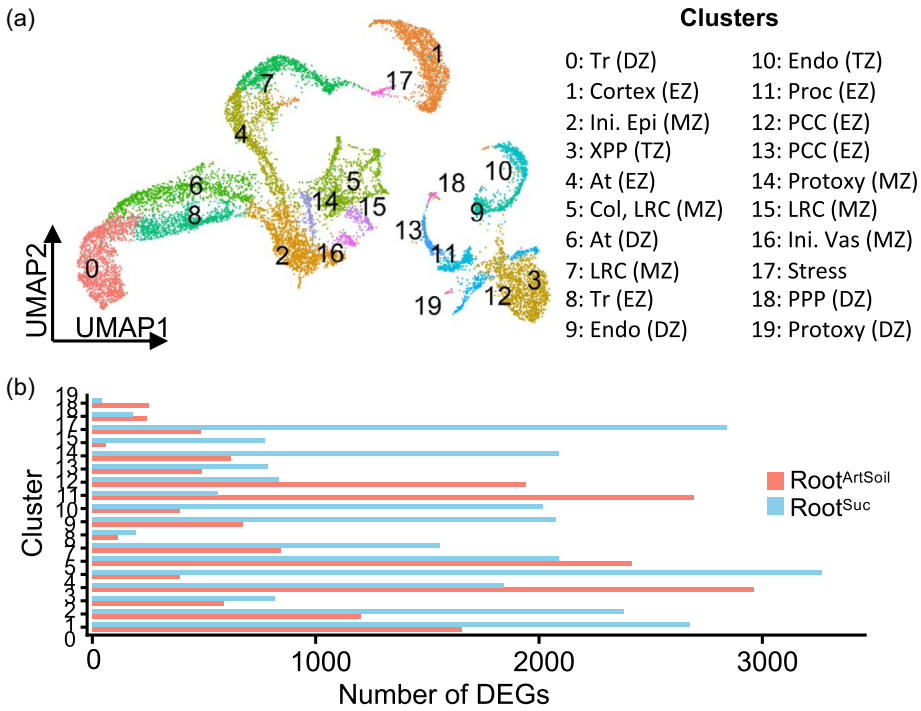

Figure 5. Single-cell transcriptomics of root from *A. thaliana* grown on ArtSoil (Root^{ArtSoil}).
(a) UMAP visualization of 14 100 single cells from 7-day-old *A. thaliana* roots grown on ArtSoil. UMAP projection from two independent replicates of RootArtSoil. Cell-type: At, Atrichoblast; Col, columella; Endo, endodermis; Ini, initial cells; LRC, lateral root cap; PCC, phloem companion cell; PPP, phloem pole pericycle; Proc, Procambium; Protoxy, protoxylem; Stress, protoplast-induced; Tr, trichoblast; XPP, xylem pole parenchyma. Developmental zone: DZ, differentiation zone; EZ, elongation zone; MZ, meristematic zone; TZ, transition zone.
(b) Bar plot summarizing the number of DEGs (adjusted $P < 0.05$) in each indicated cluster in RootArtSoil and RootSuc. Each bar represents a cluster; the color of the bar represents data derived from RootArtSoil or RootSuc (cluster annotation for RootArtSoil indicated in Figure 5a).

root microbiome promote plant growth (Figure 4a), they likely operate through distinct mechanisms, as reflected by their differential cell-type- and zone-specific transcriptomes.

To assess the effect of root microbiota on root defense responses at the cellular level, mRNA accumulation of pattern-recognition receptor (PRR) genes was measured in Root^{ArtSoil}. Compared to bulk root transcriptomics of gnotobiotic *A. thaliana* grown in the presence of phylogenetically diverse bacteria, fungi, and oomycetes communities (Hou et al., 2021), *FLS2, EFR, XPS1, RLP1*, and *RLP32*, which were not significantly induced in bulk transcriptomics, were significantly upregulated in a cell-type-specific manner in Root^{ArtSoil} (Figure 6a). *FLS2* was significantly upregulated in the lateral root cap, in good accordance with previous work (Zhou et al., 2020), and in a small population of procambium cells in the EZ. Among the PRRs, *EFR* was most highly and abundantly induced in the protoxylem (MZ, EZ, DZ), atrichoblast (DZ), and trichoblast (EZ). *XPS1* was predominantly upregulated in PCC (EZ) and protoxylem (MZ), *RLP1* in the MZ, whereas *RLP32* was upregulated in the protoxylem (late EZ, DZ). Notably, less than 25% of the specific root cell population showed accumulation of mRNA transcripts for the respective PRRs, suggesting masked gene induction in bulk root transcriptomics. In sum, Root^{ArtSoil}, demonstrates cell-type-specificity in PRR induction.

Since sucrose induces defense gene activation (Yamada & Mine, 2024), microbiota-induced defense gene activation was compared to that induced by sucrose. To this end, damage-induced immunity receptors and co-receptor, that is, *PEPR1, PEPR2*, and *BAK1* were traced in Root^{ArtSoil} and Root^{Suc} for their previously described role in root immunity (Jing et al., 2023; Zhou et al., 2020). While PRRs were not induced to levels comparable to those in Root^{ArtSoil} (*RLP32* was not significantly induced), *PEPR1, PEPR2*, and *BAK1* exhibited markedly higher and more abundant mRNA transcript accumulation. While approximately 25% of the ground tissue (MZ) accumulated *PEPR1* in Root^{ArtSoil}, *PEPR1* was induced in more than 75% of the QC and atrichoblast (MZ) in Root^{Suc} (Figure 6a). Similarly, *PEPR2* and *BAK1* were induced in a greater proportion of cells and to higher levels in Root^{Suc} than in Root^{ArtSoil}. Thus, comparison between Root^{ArtSoil} and Root^{Suc} indicated that sugar induces damage-triggered immune responses, which may introduce artifacts in plant–microbe interaction studies using axenic media supplemented with sucrose. Alternatively, the damage signaling pathway

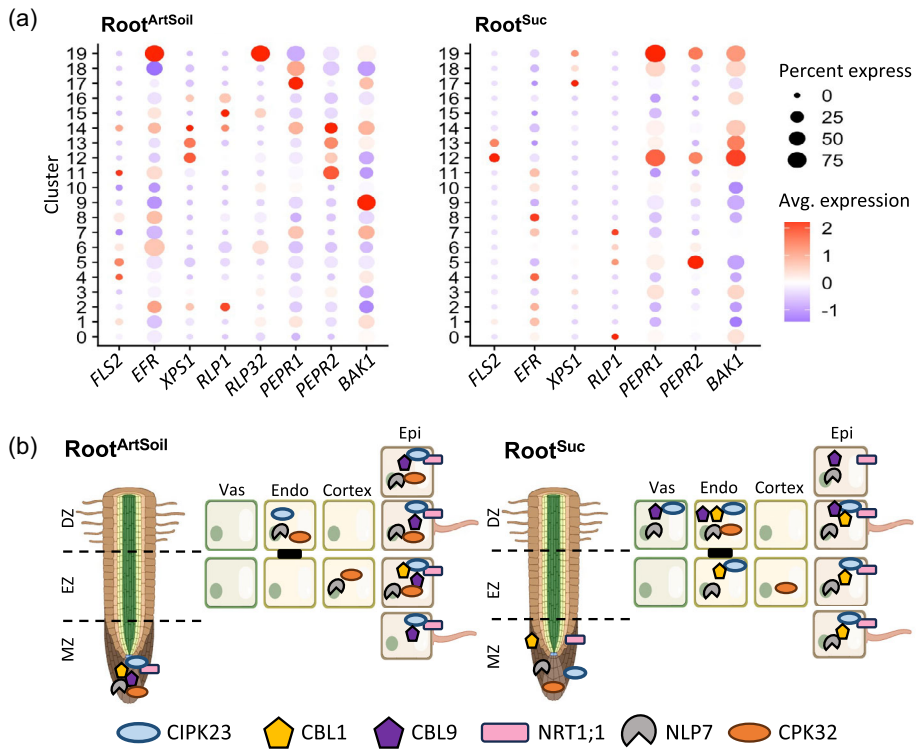

Figure 6. Microbiota-induced cell-type-specificity in immune and nitrogen signaling.
(a) Dot plots describing the percentage of each cell cluster expressing the indicated genes in RootArtSoil and RootSuc. Cell cluster for RootArtSoil described in UMAP in Figure 5a, and in Figure S4 for RootSuc. Size of dots indicates percentage of cells expressing the indicated genes; colors of dots indicate average expression of indicated genes.
(b) Cartoon depiction summarizing the presence of mRNA transcripts of six representative nitrogen uptake signaling components in roots of plants grown on ArtSoil or media with sucrose supplementation (Shahan et al., 2022). Epi, epidermis; Endo, endodermis; Vas, vasculature.

involving PEPRs may be implicated in unidentified non-immunity processes.

The microbiota influences plant nutrient status and has been implicated in promoting plant growth via nitrogen uptake (Calvo et al., 2019; Hernández-Reyes et al., 2022; Kechid et al., 2013; Mantelin, 2003). In nodulating plants, initial interaction between host and nitrogen-fixing bacteria occurs at the root hair epidermis (Oldroyd et al., 2011). To investigate whether microbiota-mediated nitrogen uptake could be cell-type-specific in *A. thaliana*, the nitrogen signaling pathway was traced in Root^{ArtSoil}. Among the nitrate transporters, only *NRT1.1* was upregulated in the root, specifically in the trichoblast and atrichoblast in the EZ and DZ (Figure S4). Following nitrate perception, a signaling cascade involving CIPK23 and its interacting partners CBL1 and CBL9 activates the master regulator NLP7 transcription factor (Huang et al., 1996; Liu et al., 2017; Liu, Liu, et al., 2022; Ródenas & Vert, 2021). *CIPK23* and *CBL9* co-expressed with *NRT1.1* in the atrichoblast and trichoblast in the EZ and DZ, whereas *CIPK23* and *CBL1* co-expressed with *NRT1;1* in the atrichoblast in the DZ (Figure 6b; Figure S4). While both *CBL1* and/or *CBL9* co-expressed with *CIPK23* and *NLP7* in the atrichoblast and trichoblast throughout the three root zones, *CBL1* accumulation was detected only in the EZ, suggesting root zone-specificity for *CBL1/CIPK23/NLP7* interaction. CPK32 translocates into the nucleus to activate NLP7 (Konishi et al., 2021). Transcripts of *NLP7* were detected in cells where *NRT1;1, CIPK23, CBL1/9,* and *NLP7* were present, suggesting a functional nitrogen signaling complex in epidermal cells in DZ and EZ. Notably, transcripts of *CIPK23, CPK32,* and *NLP7* were detected in the endodermis (DZ) and cortex (EZ) despite the absence of detectable *CBL1* or *CBL9* transcripts. Intriguingly, the co-expression of the signaling components in Root^{ArtSoil} indicates that the nitrogen signaling pathway is confined to the trichoblast and atrichoblast in the EZ and DZ, and the LRC (Figure 6b). Tracing the same nitrogen signaling module in Root^{Suc} indicated activation of the nitrogen signaling pathway in the endodermis (EZ and DZ) in addition to the trichoblast and atrichoblast. Taken together, single-cell transcriptomics of roots from *A. thaliana* grown on ArtSoil revealed cell-type-specificity in microbiota-induced immune and nitrogen transcriptional reprogramming.

ArtSoil accommodates various aqueous soil extracts and plant species

To determine whether ArtSoil is compatible with ASEs of other soils, four ASEs derived from native soils ArtSoil^{CAS}, Reijerskamp (ArtSoil^{REI}), Oranjewoud (ArtSoil^{ORJ}), and Aijen (ArtSoil^{AI}); and two commercial potting soils (i.e., soil enriched with macronutrients), Bedding Plant substrate (ArtSoil^{BP}, https://klasmann-deilmann.com/de/anwendungsfelder/beet-und-balkonpflanzen) and Düsovit (ArtSoil^{DUS}, https://www.duesovit.de/blumenerde.htm), were tested. Four-week-old plants grown on ArtSoil^{CAS}, ArtSoil^{BP}, or ArtSoil^{DUS} were significantly larger, whereas plants grown on ArtSoil^{AI}, ArtSoil^{ORJ}, or ArtSoil^{REI} were not significantly different from plants grown on MS −suc (Figure 7a,b). Plant growth on ArtSoil was compared with that on the respective native soils (Figure 7b). At 4 weeks old, plant growth was comparable between ArtSoil and native soil except for REI and OR. ArtSoil^{OR} but not native OR soil supported plant growth, whereas native REI soil but not ArtSoil^{REI} supported plant growth. Since soil pH is an important soil property that can affect plant growth and microbial interactions (Rousk et al., 2010; Xiong et al., 2024), we posit that autoclaving soil for ASE preparation could alter the pH of ASE and, consequently, the microbial community and plant growth. The pH of both REI and OR changed after autoclaving (Figure S5), potentially affecting plant growth. Noteworthy, the pH of DUS was altered by autoclaving; however, the phenotype remained unaffected.

To disentangle the possible effects of nutrients from microbiota on plants grown on ArtSoil, 2-week-old plants grown on sterile ArtSoil (i.e., without fresh soil solution, Figure 1) were evaluated. We posit that younger plants are more sensitive to nutrient availability due to higher metabolic demand for vegetative growth. Shoot fresh mass from plants grown on sterile ArtSoil with various ASE was significantly larger than plants grown in MS −suc (Figure 7c), indicating that ASEs contribute to plant growth. To determine whether soil nutrient content could contribute to the phenotypic differences of plants grown on ArtSoil, the nutrient contents of the soil pre- and post-autoclave (i.e., fresh soils and ASEs) were determined via inductively coupled plasma mass spectrometry (ICP-MS). The nutrient concentrations were not significantly different between fresh soil and ASEs, except for copper, vanadium, and chromium in BP, DUS, and OR, which increased in ASEs (Figure S5A, Table S1). Notably, plant growth promotion was not correlated with the increase in copper, vanadium, and chromium in ASE (Figure 7a,b). Variation in shoot fresh mass among plants grown on different ASEs on sterile ArtSoil was lower than on non-sterile ArtSoil, suggesting ASE-specific microbial influence on plant growth. Since the foundational media for ArtSoil (i.e., ½ MS) provides the essential nutrients for plant growth, we postulate that the soil microbiota and trace nutrients carried over from the ASE contribute to differences in plant growth (Anderson, 1956; Hewitt, 1951; Kumar et al., 2021). Taken together, plant growth assay on sterile ArtSoil indicated that plant growth phenotype is attributed to the presence of soil microbial community, and traces of nutrients carried over from ASE. In sum, by investigating various ASEs, ArtSoil was able to uncouple plant growth promotion conferred by microbiota from nutrients, providing opportunities for future mechanistic investigations.

To test the applicability of ArtSoil on other plant species, the growth of *Oryza sativa* ssp. *Japonica* cv. Kitaake on MS +/− suc was compared with rice plants grown on ArtSoil prepared using ASE from rice agricultural soil. Consistent with *A. thaliana*, the average shoot lengths of rice seedlings grown on MS + suc or on ArtSoil were higher compared to seedlings grown on MS −suc (Figure 7d). The shoot lengths of rice seedlings grown on MS + suc were not significantly different from those of ArtSoil. To assess the capability of ArtSoil to support plant growth relative to native soil, the shoot length of rice seedlings cultivated on ArtSoil was compared to that of seedlings grown on the corresponding agricultural soil. The average shoot length of rice seedlings grown on ArtSoil was not significantly different compared to rice seedlings grown on the agricultural soil (Figure 7d). Thus, ArtSoil is applicable beyond *A. thaliana* and supports plant growth comparable to that on native soil.

DISCUSSION

Development of the ArtSoil

ArtSoil was developed to conserve soil microbial communities and soil edaphic factors in the growth medium, thereby enabling plant cultivation under environments resembling the soil environment. ArtSoil was developed based on the criteria: (i) readily available, (ii) ease of use, and (iii) customizable. ArtSoil requires materials and apparatus readily available in most laboratories and commonly used for plant growth, that is, Petri dishes, growth media, and soil. ArtSoil does not require special tools or techniques for assembly and is similar to the preparation of standard growth media. Soil edaphic factors, that is, pH and trace nutrients are introduced into the growth medium via sterile ASE. The soil microbial population is subsequently introduced in controlled quantities using fresh soil. ArtSoil is compatible with most soils tested and is, therefore, customizable to the user's choice of soil. Due to differences between soil properties, it is however important to either optimize the dilution of ASE and/or to test a set ASEs from different soils. Cultivation on ArtSoil does not differ from growing plants in other plate-based growth systems, for example, in a growth chamber under controlled conditions.

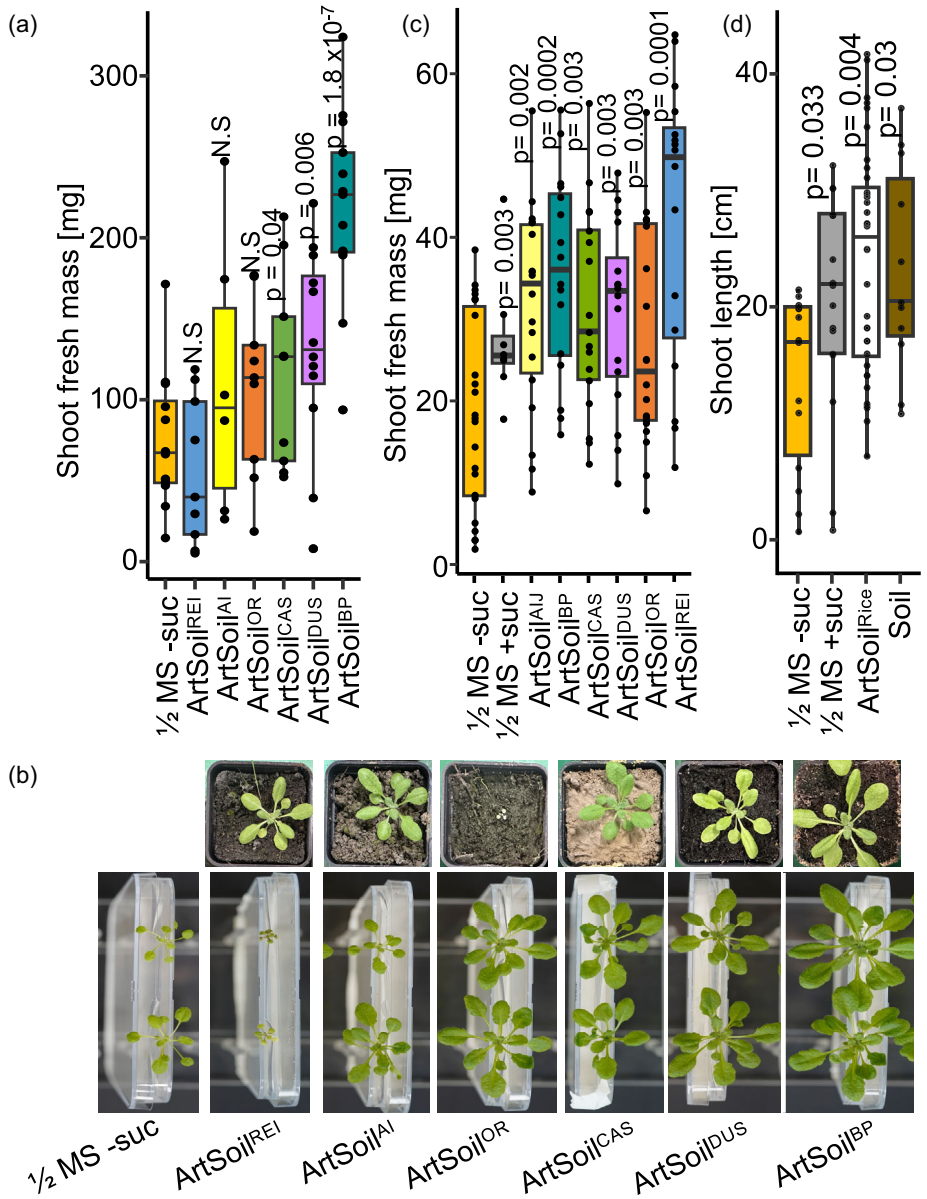

Figure 7. ASEs influence plant growth on ArtSoil.
(a) Shoot fresh mass and phenotype and of 4-week-old *A. thaliana* grown on ArtSoil with indicated ASEs. Assay was repeated twice, using independent ASE batches to ensure data reproducibility, $N > 20$. *P* value calculated via Student's *t*-test against ½ MS without sucrose supplementation (½ MS −suc). N.S., not significant.
(b) Phenotypic comparison of corresponding 4-week-old plants in (A) grown on indicated ASEs with plants grown directly on corresponding soil. Assay repeated three times, $N > 10$.
(c) Shoot fresh mass of 2-week-old *A. thaliana* grown on sterile ArtSoil with indicated ASEs. Assay was repeated three times using independent ASE batches to ensure data reproducibility, $N > 20$. *P* value calculated via Student's *t*-test against ½ MS without sucrose supplementation (½ MS −suc). N.S., not significant. The top and bottom boundaries of each boxplot indicate the first and third quartiles, the center line indicates the median, and the whiskers represent 1.5× the interquartile range from the first and third quartiles.
(d) Total shoot length of 2-week-old *O. sativa* seedlings grown on ½ MS with or without sucrose supplementation, on ArtSoil with rice agricultural soil (ArtSoil-Rice), and the rice agricultural soil. Assay was repeated at least twice, $N > 20$. *P* value calculated via Wilcoxson test against ½ MS without sucrose supplementation (½ MS −suc). The top and bottom boundaries of each boxplot indicate the first and third quartiles, the center line indicates the median, and the whiskers represent 1.5× the interquartile range from the first and third quartiles.

ArtSoil for spatial characterization of the root

Though various plant growth systems have been developed for microbiota studies (Garrido-Oter et al., 2018; Korenblum et al., 2020; Kremer et al., 2021), a system that enables spatial profiling of the root microbiota has not been established prior to ArtSoil and CD-Rhizotron (Loo

et al., 2024). Using ArtSoil and CD-Rhizotron, we previously profiled the spatial distribution of root microbiota and demonstrated that the spatial distribution of microbes along the longitudinal axis of *A. thaliana* root is not homogeneous (Loo et al., 2024). Technological advancements enable the investigation of plant responses at single-cell resolution (Denyer et al., 2019; Jean-Baptiste et al., 2019; Ryu et al., 2019). Single-cell sequencing technology has revealed heterogeneity in *A. thaliana* leaf transcription profiles, size and composition of local microbial populations in response to pathogen infection (Nobori et al., 2025; Saarenpää et al., 2023; Zhu et al., 2023). Similar to the leaf, *A. thaliana* root exhibits differential responses to microbial molecular patterns (Emonet et al., 2021; Zhou et al., 2020). Single-cell transcriptomics of *A. thaliana* roots have long been limited to sterile conditions due to the lack of suitable growth media, which hindered analyses in the presence of root microbiota, for example, difficulties in harvesting young seedlings grown on soil without damaging roots, and in obtaining suitable protoplasts (free from soil particles) for subsequent cell sorting. ArtSoil enables single-cell resolution studies of microbiota-associated roots by facilitating large-scale cultivation of seedlings required to obtain sufficient protoplasts for single-cell sequencing. The cleaner roots derived plants grown on ArtSoil may also facilitate embedding and microsectioning for spatial transcriptomics, for example, molecular cartography. Along with bacterial *in situ* hybridization, ArtSoil could be used for studying root responses to microbes at the single-cell level and examining transcriptomic differences between colonized and uncolonized cells. ArtSoil avoids the use of sucrose, and therefore will likely yield expression profiles more similar to those under native soil conditions. ArtSoil thus enables effective correlation of root gene expression profiles with microbiota colonization at the single-cell level.

An increasing number of studies have shown strong associations between root exudate composition and microbiota colonization (Koprivova & Kopriva, 2022; Korenblum et al., 2020; McLaughlin et al., 2023; Micallef et al., 2009). The state-of-the-art method for root exudate collection involves growing plants in nutrient media, followed by transferring plants to distilled water or buffers. Nutrient media are sampled at specified time intervals and compared with a control (Döll et al., 2024; Oburger et al., 2013). Transferring plants from nutrient media to distilled water alters exudation patterns due to increased analyte gradients, hypoosmotic shock, and possibly even plant cell lysis (Aulakh et al., 2001; Ayers & Thornton, 1968; Oburger et al., 2013). For instance, transferring maize seedlings from nutrient media to water alters the deposition rate of metabolites along the root zones and the rate of metabolite transfer across root growth zones (Walter et al., 2003). Root exudate collection using state-of-the-art methods thus masks metabolite heterogeneity along and across the root (Kranawetter et al., 2021; Loo et al., 2024; Moussaieff et al., 2013). Since ArtSoil allows access to the root, metabolite blotting techniques could allow spatiotemporal root exudate studies without the side effects associated with hydroponic systems and environmental shock during exudate sampling.

Limitations of ArtSoil

Due to the strong preference of microbes for sugar (Estrela et al., 2021; Schäfer et al., 2023), ArtSoil is unsuitable for assays requiring media with sucrose supplementation, for example, to rescue mutant phenotypes. Sucrose in the media will lead to microbial overgrowth/overcolonization of plants, potentially causing seedling death. ArtSoil may be unsuitable for research focused on nutrient depletion, unless the concentration of MS medium/nutrients is revised. Since ArtSoil encompasses nutrients from soil, ASE-derived nutrients in ArtSoil cannot be easily manipulated. An additional alternative could be to use soils with limited nutrient-of-interest and exogenously apply the nutrient-of-interest to the desired concentration, or use nutrient-depleting methods.

Among the six soils tested on ArtSoil, the growth of plants from four ArtSoil samples reflected the growth phenotype of their corresponding native soils. Variations in soil nutrients and pH levels before and after autoclaving may account for the observed changes in growth phenotype. In this study, both soil nutrients and pH were analyzed. However, numerous factors could influence differences in plant growth, including, but not limited to, soil microbiota incompatibility between the soil and ArtSoil. Microbiota analysis conducted on ArtSoil^{CAS} demonstrated compatibility between the soil and ArtSoil. However, this was not examined for other soils. Consequently, as not all soils produced optimal growth, users are advised to use a dilution series and test ASE from their soil of choice by comparing the phenotypes of plants cultivated on native soil, MS $\pm$ suc, and/or ArtSoil with ASE derived from the potting soil used in this study.

Limitations of the study

This study demonstrated that autoclaving soil increased the concentration of copper, vanadium, and chromium in three out of six soils tested (Figure S5). Since increases in copper, vanadium, and chromium in post-autoclave soils were not observed across all six soil samples examined, it is likely that the increases were due to procedural factors. Autoclaving may affect the physical state of the soil, thereby improving extractability. Conversely, autoclaving may increase nutrient solubility, thereby improving plant adsorption. In the latter case, plant growth on ArtSoil will be affected. However, plant growth promotion was not reflected in ASE with or without increases in copper,

vanadium, and chromium. The effects of autoclaving soil on plant growth should be interpreted with caution. Future studies comparing elements in plants grown on fresh and autoclaved soil would provide better resolution.

In conclusion, we introduce ArtSoil as an alternative growth medium that emulates the soil environment compared to the typically used conventional synthetic media. ArtSoil captures soil edaphic factors and microbiota that support plant growth without requiring sucrose supplementation. We provide users with guidelines backed by empirical data to determine the most suitable ArtSoil parameters for the user's experiment design. We demonstrated the application of ArtSoil in deciphering root-microbe transcriptome rewiring at the cellular level, and in spatial microbiota profiling (Loo et al., 2024). We demonstrate the use of ArtSoil to grow *A. thaliana* and rice plants, and speculate on broader applications for various plant species. In addition to characterizing root microbiota, ArtSoil can be used for a more comprehensive study of microbe–microbe–plant tripartite interactions where activities of pathogenic and/or beneficial microbes can be examined in the presence of the plant and its natural microbiota, in an ecologically relevant growth environment. ArtSoil can also be used to preselect the optimal synthetic community for use in other gnotobiotic systems. Finally, we recommend ArtSoil for laboratory assays aimed at physiological relevance to avoid artifacts/side effects associated with exogenous sucrose addition.

MATERIALS AND METHODS

Plant growth conditions

Refer to supplementary Methods for detailed protocol of ArtSoil preparation. For all experiments, *A. thaliana* wild-type Col-0 plants were used. Seeds were surface-sterilized in a 10% bleach solution supplemented with Triton X-100 for 10 min, followed by four washes with sterile water. Sterilized seeds were resuspended in sterile water and stratified in the dark at 4°C for at least 3 days prior to sowing. Plants were grown at 23°C with a 10-h day/14-h dark cycle and the light intensity of 25 or 120 μmol m^{-2} s^{-1}, according to the experimental setup.

Plant phenotyping

Total root length (TRL) was measured weekly for 4 weeks. At every measurement, images of the plates where seeds were sown were captured using a flatbed scanner (Epson Perfection V850 Pro). TRL was measured using the FIJI software, using the "free-hand draw" tool. Roots were traced, and the length was measured using the "measure" tool. The scale was calibrated to centimeters. The TRL is the sum of the length of the main and lateral roots developed by a single plant. For shoot fresh mass, the shoots were cut at the hypocotyl using tissue scissors. Shoots were tapped dry before weighing using an analytical scale.

Root protoplast isolation

Root protoplasts were isolated following a protocol adapted from Birnbaum et al. (2003), optimized for single-cell RNA sequencing. Seven-day-old *A. thaliana* Col-0 seedlings grown on ArtSoil were harvested by cutting approximately 1.5 cm from the root tip with a razor blade. Roots were rinsed in protoplast buffer (0.6 M mannitol, 0.1 M KCl, 0.02 M $MgCl_2$, 0.02 M $CaCl_2$, 0.08 M MES, and 0.1% BSA (Sigma-Aldrich), adjusted to pH 5.5 with 0.1 M Tris–HCl) for approximately 5 min to remove debris and surface microbes. The roots were transferred into 5 mL of freshly prepared enzyme solution containing 1.5% Cellulase R-10 and 0.1% Pectolyase (Duchefa Biochemie) dissolved in root protoplast buffer composed of 0.6 M mannitol, 0.1 M KCl, 0.02 M $MgCl_2$, 0.02 M $CaCl_2$, 0.08 M MES, and 0.1% BSA (Sigma-Aldrich), adjusted to pH 5.5 with 0.1 M Tris–HCl. Roots were digested at 26°C for 2 h with gentle shaking (200 rpm) on an orbital shaker. After digestion, the protoplast suspension was passed through a 100 μm nylon mesh filter and rinsed with 1–5 mL of wash buffer. Cells were centrifuged for 10 min at 500***g*** at 4°C. The supernatant was carefully removed, and the pellet was resuspended in 10 mL of wash buffer. This washing step was repeated once, and the final pellet was resuspended in ≤ 500 μL of the same buffer. Protoplasts were visually inspected under a light microscope, and, if necessary, residual debris was removed by an additional washing step. The cell suspension was passed through a 40 μm cell strainer (Corning). Protoplasts were stained with 4% Trypan blue and viable cells were quantified using a hemocytometer. The final concentration was adjusted to 500–1000 cells/μL.

Single cell library generation

A total of approximately 8000 and approximately 6100 single cells were generated on the 10X Chromium Controller system for single-cell droplet library generation utilizing the Chromium Single Cell 3′ GEM-X Reagent Kit v4 (10X Genomics, Pleasanton, CA, USA) according to manufacturer's instructions. Sequencing was carried out on a NextSeq2000 system (Illumina Inc. San Diego, USA) with a mean sequencing depth of approximately 25 000 reads/cell.

Processing of 10X genomics single cell data

Raw sequencing data was processed using the 10X Genomics CellRanger software (v9.0.1). Raw BCL-files were demultipexed and processed to Fastq-files using the CellRanger *mkfastq* pipeline. Alignment of reads to the *A. thaliana* TAIR10_59 genome build and UMI counting was performed via the CellRanger *count* pipieline to generate a gene-barcode matrix. Further analyses were carried out with the Seurat v5.1.0 R package (Butler et al., 2018; Hao et al., 2021; Stuart et al., 2019). Initial quality control consisted of removal of cells with fewer than 200 detected genes as well as removal of genes expressed in less than three cells. Cell doublets have been removed from the dataset using DoubletFinder v2.0 (McGinnis et al., 2019). Normalization has been carried out utilizing SCTransform. Dimensional reduction of the dataset was achieved by Principal Component analysis (PCA) based on identified variable genes and subsequent UMAP embedding. The number of meaningful Principal Components (PC) was selected by ranking them according to the percentage of variance explained by each PC, plotting them in an "Elbow Plot" and manually determining the number of PCs that represent the majority of variance in the dataset. Cells were clustered using the graph-based clustering approach implemented in Seurat. Markers defining each cluster as well as differential gene expression between different clusters were calculated using a Wilcoxon rank sum test which is implemented in Seurat.

Soil ICP-MS analysis

Fresh or autoclaved soil samples were dried in a 60°C oven for 48 h. The total mineral content was determined by inductively

coupled plasma mass spectrometry (ICP-MS) using an Agilent 7700 system (Waldbronn, Germany). To 100 mg homogenized soil, 500 μL of 30% HNO_3 was added and let soak for 2–3 h. Another 500 μL of 30% HNO_3 was added, and the samples were placed overnight in a water bath at 65°C. Afterward, the samples were boiled at 95°C for 30 min. After cooling down the sample to room temperature, 200 μL of 30% H_2O_2 were added and boiled again for 30 min at 95°C. A 8.8 mL of water was added to reach a final volume of about 10 mL. The samples were kept overnight at 4°C. Particles were spun down at 7000 g, 4°C for 1 h, or at 3500 G for 3 h. A 0.8 mL of supernatant was mixed with 3.2 mL of 2% HNO_3. The elemental concentration was determined using the Agilent 7700 ICP-MS following the manufacturer's instructions.

Root microbiota profiling

Total DNA was extracted using the NucleoSpin Soil Mini kit for DNA from soil (Macherey-Nagel GmbH & Co. KG, Düren, Germany) following instructions from the manufacturers. DNA samples were eluted in 50 μL nuclease-free water and used for microbial community profiling. DNA samples were used in a two-step PCR amplification protocol using primers targeting the V4-V7 16S rRNA region (799F: AACMGGATTAGATACCCKG; 1192R: ACGTCATCCCCACCTTCC) using 2 U DFS-Taq DNA polymerase, 1× incomplete buffer (Bioron GmbH, Ludwigshafen, Germany), 2 mM MgCl2, 0.3% BSA, 0.2 mM dNTPs (Life technologies GmbH, Darmstadt, Germany), and 0.3 μM forward and reverse primers. PCR was performed using the following parameters: 94°C/2 min, 94°C/30 sec, 55°C/30 sec, 72°C/30 sec, 72°C/10 min for 25 cycles. PCR products were pooled, end-repaired, A-tailed, and ligated with Illumina adapters. Amplicon concentration was determined fluorescently (Quant-iT™ PicoGreen™, Invitrogen), and equivalent DNA amounts of each of the barcoded amplicons were pooled in one library. The final library concentration was estimated fluorescently (Quantus™ Fluorometer, Promega). Paired-end Illumina sequencing was performed in-house using the MiSeq sequencer and custom sequencing primers at the Max Planck Institute for Plant Breeding Research.

For microbiota turnover, the extracted DNA was sequenced using Oxford Nanopore Technologies with the 16S Barcoding Kit (SQK-16S114.24) (Oxford Nanopore Technologies, United Kingdom). Library preparation was performed following the manufacturer's protocol. Due to low DNA quality ratios, the number of amplification cycles for full-length 16S rRNA gene amplification was increased to 60. DNA concentration was quantified using the Qubit dsDNA BR Assay Kit (Thermo Fisher Scientific, USA), and successful amplification was verified by electrophoresis on a 0.8% agarose gel. Sequencing was carried out on a MinION device using R10.4.1 FLO-MIN114 flow cells (Oxford Nanopore Technologies, UK). Raw sequencing data were basecalled with Dorado (v1.3.0) using the model dna_r10.4.1_e8.2_400bps_sup@v5.2.0 and specifying the parameter --kit-name SQK-16S114-24. Demultiplexing was performed with Dorado demux (v1.3.0) using the --no-classify and --emit-summary options. Demultiplexed BAM files were filtered to retain reads with a minimum Q-score of 15 by SAMtools view (v1.20) with the parameters -e "[qs] ≥15" and converted to FASTQ format using SAMtools fastq (v1.20) (Danecek et al., 2021). Sequencing statistics of demultiplexed FASTQ data were generated with SeqKit stats (v2.9.0) using the --all option (Shen et al., 2024). Full-length 16S rRNA amplicon sequences were processed for taxonomic classification using Kraken2 (v2.1.1) with the SILVA 138.2 database prebuilt for Kraken2. Kraken2 was run with 16 threads and a confidence threshold of 0.1. Taxonomic counts were extracted directly using the rank field in the report. Classifications were performed using $k = 35$. Per-sample counts were merged into matrices for relative abundance analyses and visualization.

AUTHOR CONTRIBUTIONS

EL: Conception; EL, VK, and HA: Writing; HA, TG, LM, and EL: Plant phenotyping; VJ-R, PD, and EL: Microbiota; VK, EL, and TL: Single-cell transcriptomics; VK, SM, and EL: Soil analysis.

ACKNOWLEDGMENTS

This research has been supported by the Deutsche Forschungsgemeinschaft (DFG, German Research Foundation) under Germany's Excellence Strategy–EXC-2048/1 (project ID 390686111), DFG project ID 391465903/GRK 2466, Collaborative Research Center MibiNet (CRC 1535), funded by the Deutsche Forschungsgemeinschaft (DFG, German Research Foundation, Project ID 458090666) and the Alexander von Humboldt Foundation (AvH professorship to Wolf Frommer). Computational and sequencing infrastructure and support were provided by the Centre for Information and Media Technology and the lab of Björn Usadel (Institute for Biological Data Science) at Heinrich Heine University Düsseldorf. We thank the lab of Bart Thomma (Universität zu Köln) and Marco Romani (Ente Nazionale Risi) for contributing soil samples, Dominik Brilhaus for data management, Wolf Frommer for scientific discussions, and the reviewers for constructive comments.

CONFLICT OF INTEREST

The authors declare no competing interests.

DATA AVAILABILITY STATEMENT

Data produced in this work have been deposited in DataPLANT under the following https://doi.org/10.60534/83npp-dhx68.

SUPPORTING INFORMATION

Additional Supporting Information may be found in the online version of this article.

Method S1. Detailed protocol for the preparation of ArtSoil.

Figure S1. Microbial load and turnover in ArtSoil^{CAS}.

Figure S2. Time-series quantification of total root length of *A. thaliana* grown under optimal or suboptimal light conditions on ArtSoil, ½ MS with or without sucrose supplementation.

Transcriptomics analyses for Root^{ArtSoil}, Root^{Suc}, and Root^{NoSuc}.

Figure S3. Compatibility of single-cell transcriptomics of roots from *A. thaliana* grown on ArtSoil or MS + suc.

Figure S4. Cell-type-specific induction of nitrogen signaling pathway in the roots of *A. thaliana* grown on ArtSoil or MS + suc.

Figure S5. Elemental analysis of soils before and after autoclaving.

Table S1. Soil elemental analysis for the amount (mg/kg) of each nutrient found in respective soil sample.

REFERENCES

Anderson, A.J. (1956) Molybdenum as a fertilizer. In: *Advances in Agronomy*. Elsevier, pp. 163–202. Available from: https://doi.org/10.1016/S0065-2113(08)60689-6

Aulakh, M.S., **Wassmann, R.**, **Bueno, C.**, **Kreuzwieser, J.** & **Rennenberg, H.** (2001) Characterization of root exudates at different growth stages of ten

rice (*Oryza sativa* L.) cultivars. *Plant Biology*, **3**, 139–148. Available from: https://doi.org/10.1055/s-2001-12905

Ayers, W.A. & **Thornton, R.H.** (1968) Exudation of amino acids by intact and damaged roots of wheat and peas. *Plant and Soil*, **28**, 193–207. Available from: https://doi.org/10.1007/BF01880238

Bakker, P.A.H.M., **Pieterse, C.M.J.**, **De Jonge, R.** & **Berendsen, R.L.** (2018) The soil-borne legacy. *Cell*, **172**, 1178–1180. Available from: https://doi.org/10.1016/j.cell.2018.02.024

Berendsen, R.L., **Vismans, G.**, **Yu, K.**, **Song, Y.**, **De Jonge, R.**, **Burgman, W.P.** ***et al.*** (2018) Disease-induced assemblage of a plant-beneficial bacterial consortium. *The ISME Journal*, **12**, 1496–1507. Available from: https://doi.org/10.1038/s41396-018-0093-1

Birnbaum, K., **Shasha, D.E.**, **Wang, J.Y.**, **Jung, J.W.**, **Lambert, G.M.**, **Galbraith, D.W.** ***et al.*** (2003) A gene expression map of the *Arabidopsis* root. *Science*, **302**, 1956–1960. Available from: https://doi.org/10.1126/science.1090022

Bodenhausen, N., **Bortfeld-Miller, M.**, **Ackermann, M.** & **Vorholt, J.A.** (2014) A synthetic community approach reveals plant genotypes affecting the phyllosphere microbiota. *PLoS Genetics*, **10**, e1004283. Available from: https://doi.org/10.1371/journal.pgen.1004283

Bulgarelli, D., **Rott, M.**, **Schlaeppi, K.**, **van Ver Loren Themaat, E.**, **Ahmadinejad, N.**, **Assenza, F.** ***et al.*** (2012) Revealing structure and assembly cues for Arabidopsis root-inhabiting bacterial microbiota. *Nature*, **488**, 91–95. Available from: https://doi.org/10.1038/nature11336

Bulgarelli, D., **Schlaeppi, K.**, **Spaepen, S.**, **van Ver Loren Themaat, E.** & **Schulze-Lefert, P.** (2013) Structure and functions of the bacterial microbiota of plants. *Annual Review of Plant Biology*, **64**, 807–838. Available from: https://doi.org/10.1146/annurev-arplant-050312-120106

Butler, A., **Hoffman, P.**, **Smibert, P.**, **Papalexi, E.** & **Satija, R.** (2018) Integrating single-cell transcriptomic data across different conditions, technologies, and species. *Nature Biotechnology*, **36**, 411–420. Available from: https://doi.org/10.1038/nbt.4096

Calvo, P., **Zebelo, S.**, **McNear, D.**, **Kloepper, J.** & **Fadamiro, H.** (2019) Plant growth-promoting rhizobacteria induce changes in *Arabidopsis thaliana* gene expression of nitrate and ammonium uptake genes. *Journal of Plant Interactions*, **14**, 224–231. Available from: https://doi.org/10.1080/17429145.2019.1602887

Carlström, C.I., **Field, C.M.**, **Bortfeld-Miller, M.**, **Müller, B.**, **Sunagawa, S.** & **Vorholt, J.A.** (2019) Synthetic microbiota reveal priority effects and keystone strains in the Arabidopsis phyllosphere. *Nature Ecology & Evolution*, **3**, 1445–1454. Available from: https://doi.org/10.1038/s41559-019-0994-z

Carrión, V.J., **Perez-Jaramillo, J.**, **Cordovez, V.**, **Tracanna, V.**, **De Hollander, M.**, **Ruiz-Buck, D.** ***et al.*** (2019) Pathogen-induced activation of disease-suppressive functions in the endophytic root microbiome. *Science*, **366**, 606–612. Available from: https://doi.org/10.1126/science.aaw9285

Castrillo, G., **Teixeira, P.J.P.L.**, **Paredes, S.H.**, **Law, T.F.**, **De Lorenzo, L.**, **Feltcher, M.E.** ***et al.*** (2017) Root microbiota drive direct integration of phosphate stress and immunity. *Nature*, **543**, 513–518. Available from: https://doi.org/10.1038/nature21417

Chen, L.-Q., **Lin, I.W.**, **Qu, X.-Q.**, **Sosso, D.**, **McFarlane, H.E.**, **Londoño, A.** ***et al.*** (2015) A cascade of sequentially expressed sucrose transporters in the seed coat and endosperm provides nutrition for the Arabidopsis embryo. *Plant Cell*, **27**, 607–619. Available from: https://doi.org/10.1105/tpc.114.134585

Chesneau, G., **Herpell, J.**, **Garrido-Oter, R.** & **Hacquard, S.** (2025) From synthetic communities to synthetic ecosystems: exploring causalities in plant–microbe–environment interactions. *New Phytologist*, **245**, 496–502. Available from: https://doi.org/10.1111/nph.20250

Claeijs, N. & **Vissenberg, K.** (2022) Phenotypic effect of growth media on Arabidopsis thaliana root hair growth. *Plant Signaling & Behavior*, **17**, 2104002. Available from: https://doi.org/10.1080/15592324.2022.2104002

Cook, K.L., **Garland, J.L.**, **Layton, A.C.**, **Dionisi, H.M.**, **Levine, L.H.** & **Sayler, G.S.** (2006) Effect of microbial species richness on community stability and community function in a model plant-based wastewater processing system. *Microbial Ecology*, **52**, 725–737. Available from: https://doi.org/10.1007/s00248-006-9105-1

Danecek, P., **Bonfield, J.K.**, **Liddle, J.**, **Marshall, J.**, **Ohan, V.**, **Pollard, M.O.** ***et al.*** (2021) Twelve years of SAMtools and BCFtools. *GigaScience*, **10**, giab008. Available from: https://doi.org/10.1093/gigascience/giab008

Daniel, A.I., **Fadaka, A.O.**, **Gokul, A.**, **Bakare, O.O.**, **Aina, O.**, **Fisher, S.** ***et al.*** (2022) Biofertilizer: the future of food security and food safety. *Microorganisms*, **10**, 1220. Available from: https://doi.org/10.3390/microorganisms10061220

de Souza, R., **Ambrosini, A.** & **Passaglia, L.M.P.** (2015) Plant growth-promoting bacteria as inoculants in agricultural soils. *Genetics and Molecular Biology*, **38**, 401–419. Available from: https://doi.org/10.1590/S1415-475738420150053

Denyer, T., **Ma, X.**, **Klesen, S.**, **Scacchi, E.**, **Nieselt, K.** & **Timmermans, M.C.P.** (2019) Spatiotemporal developmental trajectories in the Arabidopsis root revealed using high-throughput cingle-cell RNA sequencing. *Developmental Cell*, **48**, 840–852.e5. Available from: https://doi.org/10.1016/j.devcel.2019.02.022

Dini-Andreote, F., **Wells, D.M.**, **Atkinson, J.A.**, **Atkinson, B.S.**, **Finkel, O.M.** & **Castrillo, G.** (2025) Microbial drivers of root plasticity. *New Phytologist*, **248**, 52–67. Available from: https://doi.org/10.1111/nph.70371

Döll, S., **Koller, H.** & **Van Dam, N.M.** (2024) A simple, cost-effective and optimized protocol for collecting root exudates from soil grown plants. *Rhizosphere*, **30**, 100899. Available from: https://doi.org/10.1016/j.rhisph.2024.100899

Durán, P., **Thiergart, T.**, **Garrido-Oter, R.**, **Agler, M.**, **Kemen, E.**, **Schulze-Lefert, P.** ***et al.*** (2018) Microbial interkingdom interactions in roots promote Arabidopsis survival. *Cell*, **175**, 973–983.e14. Available from: https://doi.org/10.1016/j.cell.2018.10.020

Durán, P., **Vailleau, F.** & **Roux, F.** (2025) Building microbial synthetic communities: get inspired by the design of synthetic plant communities. *New Phytologist*, **246**, 402–405. Available from: https://doi.org/10.1111/nph.70011

Edwards, J., **Johnson, C.**, **Santos-Medellín, C.**, **Lurie, E.**, **Podishetty, N.K.**, **Bhatnagar, S.** ***et al.*** (2015) Structure, variation, and assembly of the root-associated microbiomes of rice. *Proceedings. National Academy of Sciences. United States of America*, **112**, E911–E920. Available from: https://doi.org/10.1073/pnas.1414592112

Emonet, A., **Zhou, F.**, **Vacheron, J.**, **Heiman, C.M.**, **Dénervaud Tendon, V.**, **Ma, K.-W.** ***et al.*** (2021) Spatially restricted immune responses are required for maintaining root meristematic activity upon detection of bacteria. *Current Biology*, **31**, 1012–1028.e7. Available from: https://doi.org/10.1016/j.cub.2020.12.048

Estrela, S., **Sanchez-Gorostiaga, A.**, **Vila, J.C.** & **Sanchez, A.** (2021) Nutrient dominance governs the assembly of microbial communities in mixed nutrient environments. *eLife*, **10**, e65948. Available from: https://doi.org/10.7554/eLife.65948

Fan, D., **Hu, W.**, **Xu, N.**, **Seto, E.R.**, **Lagarias, J.C.**, **Chen, X.** ***et al.*** (2025) A multisensor high-temperature signaling framework for triggering daytime thermomorphogenesis in Arabidopsis. *Nature Communications*, **16**, 5197. Available from: https://doi.org/10.1038/s41467-025-60498-7

Fukami, T. (2015) Historical contingency in community assembly: integrating niches, species pools, and priority effects. *Annual Review of Ecology, Evolution, and Systematics*, **46**, 1–23. Available from: https://doi.org/10.1146/annurev-ecolsys-110411-160340

Gamborg, O.L., **Miller, R.A.** & **Ojima, K.** (1968) Nutrient requirements of suspension cultures of soybean root cells. *Experimental Cell Research*, **50**, 151–158. Available from: https://doi.org/10.1016/0014-4827(68)90403-5

Gao, J., **Sasse, J.**, **Lewald, K.M.**, **Zhalnina, K.**, **Cornmesser, L.T.**, **Duncombe, T.A.** ***et al.*** (2018) Ecosystem fabrication (EcoFAB) protocols for the construction of laboratory ecosystems designed to study plant-microbe interactions. *JoVE*, 57170. Available from: https://doi.org/10.3791/57170-v

Garrido-Oter, R., **Nakano, R.T.**, **Dombrowski, N.**, **Ma, K.-W.**, **McHardy, A.C.** & **Schulze-Lefert, P.** (2018) Modular traits of the Rhizobiales root microbiota and their evolutionary relationship with symbiotic rhizobia. *Cell Host & Microbe*, **24**, 155–167.e5. Available from: https://doi.org/10.1016/j.chom.2018.06.006

Gouda, S., **Kerry, R.G.**, **Das, G.**, **Paramithiotis, S.**, **Shin, H.-S.** & **Patra, J.K.** (2018) Revitalization of plant growth promoting rhizobacteria for sustainable development in agriculture. *Microbiological Research*, **206**, 131–140. Available from: https://doi.org/10.1016/j.micres.2017.08.016

Hao, Y., **Hao, S.**, **Andersen-Nissen, E.**, **Mauck, W.M.**, **Zheng, S.**, **Butler, A.** ***et al.*** (2021) Integrated analysis of multimodal single-cell data. *Cell*, **184**, 3573–3587.e29. Available from: https://doi.org/10.1016/j.cell.2021.04.048

Hernández-Reyes, C., **Lichtenberg, E.**, **Keller, J.**, **Delaux, P.-M.**, **Ott, T.** & **Schenk, S.T.** (2022) NIN-like proteins: interesting players in rhizobia-induced nitrate signaling response during interaction with non-legume

host *Arabidopsis thaliana*. *MPMI*, **35**, 230–243. Available from: https://doi.org/10.1094/MPMI-10-21-0261-R

Hewitt, E.J. (1951) The role of the mineral elements in plant nutrition. *Annual Review of Plant Physiology*, **2**, 25–52. Available from: https://doi.org/10.1146/annurev.pp.02.060151.000325

Hoagland, D.R. & **Armon, D.I.** (1950) *The water-culture method for growing plants without soil*. Berkeley, Calif.: College of Agriculture, University of California.

Hou, S., **Thiergart, T.**, **Vannier, N.**, **Mesny, F.**, **Ziegler, J.**, **Pickel, B.** ***et al.*** (2021) A microbiota–root–shoot circuit favours Arabidopsis growth over defence under suboptimal light. *Nature Plants*, **7**, 1078–1092. Available from: https://doi.org/10.1038/s41477-021-00956-4

Huang, N.C., **Chiang, C.S.**, **Crawford, N.M.** & **Tsay, Y.F.** (1996) CHL1 encodes a component of the low-affinity nitrate uptake system in Arabidopsis and shows cell type-specific expression in roots. *Plant Cell*, **8**, 2183–2191. Available from: https://doi.org/10.1105/tpc.8.12.2183

Huang, X.-J., **Jian, S.-F.**, **Chen, D.-L.**, **Zhong, C.** & **Miao, J.-H.** (2022) Concentration-dependent dual effects of exogenous sucrose on nitrogen metabolism in Andrographis paniculata. *Scientific Reports*, **12**, 4906. Available from: https://doi.org/10.1038/s41598-022-08971-x

Jean-Baptiste, K., **McFaline-Figueroa, J.L.**, **Alexandre, C.M.**, **Dorrity, M.W.**, **Saunders, L.**, **Bubb, K.L.** ***et al.*** (2019) Dynamics of gene expression in single root cells of *Arabidopsis thaliana*. *Plant Cell*, **31**, 993–1011. Available from: https://doi.org/10.1105/tpc.18.00785

Jing, Y., **Zou, X.**, **Sun, C.**, **Qin, X.** & **Zheng, X.** (2023) Danger-associate peptide regulates root immunity in Arabidopsis. *Biochemical and Biophysical Research Communications*, **663**, 163–170. Available from: https://doi.org/10.1016/j.bbrc.2023.04.091

Kechid, M., **Desbrosses, G.**, **Rokhsi, W.**, **Varoquaux, F.**, **Djekoun, A.** & **Touraine, B.** (2013) The <><>NRT</> 2.5</> and <><>NRT</> 2.6 genes are involved in growth promotion of *Arabidopsis* by the plant growth-promoting rhizobacterium (<sc>PGPR</sc>) strain *Phyllobacterium brassicacearum*<sc>STM</sc> 196. *New Phytologist*, **198**, 514–524. Available from: https://doi.org/10.1111/nph.12158

Kircher, S. & **Schopfer, P.** (2023) Photosynthetic sucrose drives the lateral root clock in Arabidopsis seedlings. *Current Biology*, **33**, 2201–2212.e3. Available from: https://doi.org/10.1016/j.cub.2023.04.061

Konishi, M., **Okitsu, T.** & **Yanagisawa, S.** (2021) Nitrate-responsive NIN-like protein transcription factors perform unique and redundant roles in Arabidopsis. *Journal of Experimental Botany*, **72**, 5735–5750. Available from: https://doi.org/10.1093/jxb/erab246

Koprivova, A. & **Kopriva, S.** (2022) Plant secondary metabolites altering root microbiome composition and function. *Current Opinion in Plant Biology*, **67**, 102227. Available from: https://doi.org/10.1016/j.pbi.2022.102227

Korenblum, E., **Dong, Y.**, **Szymanski, J.**, **Panda, S.**, **Jozwiak, A.**, **Massalha, H.** ***et al.*** (2020) Rhizosphere microbiome mediates systemic root metabolite exudation by root-to-root signaling. *Proceedings. National Academy of Sciences. United States of America*, **117**, 3874–3883. Available from: https://doi.org/10.1073/pnas.1912130117

Kranawetter, C., **Zeng, S.**, **Joshi, T.** & **Sumner, L.W.** (2021) A *Medicago truncatula* metabolite atlas enables the visualization of differential accumulation of metabolites in root tissues. *Metabolites*, **11**, 238. Available from: https://doi.org/10.3390/metabo11040238

Kremer, J.M., **Sohrabi, R.**, **Paasch, B.C.**, **Rhodes, D.**, **Thireault, C.**, **Schulze-Lefert, P.** ***et al.*** (2021) Peat-based gnotobiotic plant growth systems for Arabidopsis microbiome research. *Nature Protocols*, **16**, 2450–2470. Available from: https://doi.org/10.1038/s41596-021-00504-6

Kumar, S., **Kumar, S.** & **Mohapatra, T.** (2021) Interaction between macro- and micro-nutrients in plants. *Frontiers in Plant Science*, **12**, 665583. Available from: https://doi.org/10.3389/fpls.2021.665583

Kwak, M.-J., **Kong, H.G.**, **Choi, K.**, **Kwon, S.-K.**, **Song, J.Y.**, **Lee, J.** ***et al.*** (2018) Rhizosphere microbiome structure alters to enable wilt resistance in tomato. *Nature Biotechnology*, **36**, 1100–1109. Available from: https://doi.org/10.1038/nbt.4232

Li, Y., **Li, L.-L.**, **Fan, R.-C.**, **Peng, C.-C.**, **Sun, H.-L.**, **Zhu, S.-Y.** ***et al.*** (2012) Arabidopsis sucrose transporter SUT4 interacts with cytochrome b5-2 to regulate seed germination in response to sucrose and glucose. *Molecular Plant*, **5**, 1029–1041. Available from: https://doi.org/10.1093/mp/sss001

Liu, K., **Niu, Y.**, **Konishi, M.**, **Wu, Y.**, **Du, H.**, **Sun Chung, H.** ***et al.*** (2017) Discovery of nitrate–CPK–NLP signalling in central nutrient–growth networks. *Nature*, **545**, 311–316. Available from: https://doi.org/10.1038/nature22077

Liu, K.-H., **Liu, M.**, **Lin, Z.**, **Wang, Z.-F.**, **Chen, B.**, **Liu, C.** ***et al.*** (2022) NIN-like protein 7 transcription factor is a plant nitrate sensor. *Science*, **377**, 1419–1425. Available from: https://doi.org/10.1126/science.add1104

Liu, S., **Long, J.**, **Zhang, L.**, **Gao, J.**, **Dong, T.**, **Wang, Y.** ***et al.*** (2022) *Arabidopsis* sucrose transporter 4 (AtSUC4) is involved in high sucrose-mediated inhibition of root elongation. *Biotechnology & Biotechnological Equipment*, **36**, 561–574. Available from: https://doi.org/10.1080/13102818.2022.2101942

Liu, W., **Xu, H.**, **Zhou, J.**, **He, Y.**, **Zou, D.**, **Bai, Y.** ***et al.*** (2024) The plant microbiota: from theoretical advances to applications. *Fundamental Research*, S2667325824001985. Available from: https://doi.org/10.1016/j.fmre.2024.04.016

Loo, E.P.-I., **Durán, P.**, **Pang, T.Y.**, **Westhoff, P.**, **Deng, C.**, **Durán, C.** ***et al.*** (2024) Sugar transporters spatially organize microbiota colonization along the longitudinal root axis of Arabidopsis. *Cell Host & Microbe*, **32**, 543–556.e6. Available from: https://doi.org/10.1016/j.chom.2024.02.014

Lundberg, D.S., **Lebeis, S.L.**, **Paredes, S.H.**, **Yourstone, S.**, **Gehring, J.**, **Malfatti, S.** ***et al.*** (2012) Defining the core *Arabidopsis thaliana* root microbiome. *Nature*, **488**, 86–90. Available from: https://doi.org/10.1038/nature11237

Ma, K., **Ordon, J.** & **Schulze-Lefert, P.** (2022) Gnotobiotic plant systems for reconstitution and functional studies of the root microbiota. *Current Protocols*, **2**, e362. Available from: https://doi.org/10.1002/cpz1.362

Ma, K.-W., **Niu, Y.**, **Jia, Y.**, **Ordon, J.**, **Copeland, C.**, **Emonet, A.** ***et al.*** (2021) Coordination of microbe–host homeostasis by crosstalk with plant innate immunity. *Nature Plants*, **7**, 814–825. Available from: https://doi.org/10.1038/s41477-021-00920-2

Mantelin, S. (2003) Plant growth-promoting bacteria and nitrate availability: impacts on root development and nitrate uptake. *Journal of Experimental Botany*, **55**, 27–34. Available from: https://doi.org/10.1093/jxb/erh010

McGinnis, C.S., **Murrow, L.M.** & **Gartner, Z.J.** (2019) DoubletFinder: doublet detection in single-cell RNA sequencing data using artificial nearest neighbors. *Cell Systems*, **8**, 329–337.e4. Available from: https://doi.org/10.1016/j.cels.2019.03.003

McLaughlin, S., **Zhalnina, K.**, **Kosina, S.**, **Northen, T.R.** & **Sasse, J.** (2023) The core metabolome and root exudation dynamics of three phylogenetically distinct plant species. *Nature Communications*, **14**, 1649. Available from: https://doi.org/10.1038/s41467-023-37164-x

Mehlferber, E.C., **Arnault, G.**, **Joshi, B.**, **Partida-Martinez, L.P.**, **Patras, K.A.**, **Simonin, M.** ***et al.*** (2024) A cross-systems primer for synthetic microbial communities. *Nature Microbiology*, **9**, 2765–2773. Available from: https://doi.org/10.1038/s41564-024-01827-2

Micallef, S.A., **Shiaris, M.P.** & **Colón-Carmona, A.** (2009) Influence of *Arabidopsis thaliana* accessions on rhizobacterial communities and natural variation in root exudates. *Journal of Experimental Botany*, **60**, 1729–1742. Available from: https://doi.org/10.1093/jxb/erp053

Miotto, Y.E., **Da Costa, C.T.**, **Offringa, R.**, **Kleine-Vehn, J.** & **Maraschin, F.D.S.** (2021) Effects of light intensity on root development in a D-root growth system. *Frontiers in Plant Science*, **12**, 778382. Available from: https://doi.org/10.3389/fpls.2021.778382

Moussaieff, A., **Rogachev, I.**, **Malitsky, S.**, **Toal, T.W.**, **Belcher, H.**, **Yativ, M.** ***et al.*** (2013) High-resolution metabolic mapping of cell types in plant roots. *Proceedings. National Academy of Sciences. United States of America*, **110**, E1232–E1241. Available from: https://doi.org/10.1073/pnas.1302019110

Murashige, T. & **Skoog, F.** (1962) A revised medium for rapid growth and bio assays with tobacco tissue cultures. *Physiologia Plantarum*, **15**, 473–497. Available from: https://doi.org/10.1111/j.1399-3054.1962.tb08052.x

Nagel, K.A., **Lenz, H.**, **Kastenholz, B.**, **Gilmer, F.**, **Averesch, A.**, **Putz, A.** ***et al.*** (2020) The platform GrowScreen-agar enables identification of phenotypic diversity in root and shoot growth traits of agar grown plants. *Plant Methods*, **16**, 89. Available from: https://doi.org/10.1186/s13007-020-00631-3

Nobori, T., **Monell, A.**, **Lee, T.A.**, **Sakata, Y.**, **Shirahama, S.**, **Zhou, J.** ***et al.*** (2025) A rare PRIMER cell state in plant immunity. *Nature*, **638**, 197–205. Available from: https://doi.org/10.1038/s41586-024-08383-z

Northen, T.R., **Kleiner, M.**, **Torres, M.**, **Kovács, Á.T.**, **Nicolaisen, M.H.**, **Krzyżanowska, D.M.** ***et al.*** (2024) Community standards and future opportunities for synthetic communities in plant-microbiota research.

Nature Microbiology, **9**, 2774–2784. Available from: https://doi.org/10.1038/s41564-024-01833-4

Oburger, E., **Dell'mour, M.**, **Hann, S.**, **Wieshammer, G.**, **Puschenreiter, M.** & **Wenzel, W.W.** (2013) Evaluation of a novel tool for sampling root exudates from soil-grown plants compared to conventional techniques. *Environmental and Experimental Botany*, **87**, 235–247. Available from: https://doi.org/10.1016/j.envexpbot.2012.11.007

Oldroyd, G.E.D., **Murray, J.D.**, **Poole, P.S.** & **Downie, J.A.** (2011) The rules of engagement in the legume-rhizobial symbiosis. *Annual Review of Genetics*, **45**, 119–144. Available from: https://doi.org/10.1146/annurev-genet-110410-132549

Ortiz-Burgos, S. (2016) Shannon-Weaver diversity index. In: Kennish, M.J. (Ed.) *Encyclopedia of Estuaries, Encyclopedia of Earth Sciences Series*. Dordrecht: Springer, Netherlands, pp. 572–573. Available from: https://doi.org/10.1007/978-94-017-8801-4_233

Pereyra, M.E., **Murcia, M.G.**, **Borniego, M.B.**, **Assuero, S.G.** & **Casal, J.J.** (2022) EARLY FLOWERING 3 represses the nighttime growth response to sucrose in Arabidopsis. *Photochemical & Photobiological Sciences*, **21**, 1869–1880. Available from: https://doi.org/10.1007/s43630-022-00264-6

Poria, V., **Dębiec-Andrzejewska, K.**, **Fiodor, A.**, **Lyzohub, M.**, **Ajijah, N.**, **Singh, S.** ***et al.*** (2022) Plant growth-promoting bacteria (PGPB) integrated phytotechnology: a sustainable approach for remediation of marginal lands. *Frontiers in Plant Science*, **13**, 999866. Available from: https://doi.org/10.3389/fpls.2022.999866

Ródenas, R. & **Vert, G.** (2021) Regulation of root nutrient transporters by CIPK23: 'one kinase to rule them all. *Plant and Cell Physiology*, **62**, 553–563. Available from: https://doi.org/10.1093/pcp/pcaa156

Rousk, J., **Bååth, E.**, **Brookes, P.C.**, **Lauber, C.L.**, **Lozupone, C.**, **Caporaso, J.G.** ***et al.*** (2010) Soil bacterial and fungal communities across a pH gradient in an arable soil. *The ISME Journal*, **4**, 1340–1351. Available from: https://doi.org/10.1038/ismej.2010.58

Roycewicz, P. & **Malamy, J.E.** (2012) Dissecting the effects of nitrate, sucrose and osmotic potential on *Arabidopsis* root and shoot system growth in laboratory assays. *Philosophical Transactions of the Royal Society B*, **367**, 1489–1500. Available from: https://doi.org/10.1098/rstb.2011.0230

Russ, D., **Fitzpatrick, C.R.**, **Teixeira, P.J.P.L.** & **Dangl, J.L.** (2023) Deep discovery informs difficult deployment in plant microbiome science. *Cell*, **186**, 4496–4513. Available from: https://doi.org/10.1016/j.cell.2023.08.035

Ryu, K.H., **Huang, L.**, **Kang, H.M.** & **Schiefelbein, J.** (2019) Single-cell RNA sequencing resolves molecular relationships among individual plant cells. *Plant Physiology*, **179**, 1444–1456. Available from: https://doi.org/10.1104/pp.18.01482

Saarenpää, S., **Shalev, O.**, **Ashkenazy, H.**, **Carlos, V.**, **Lundberg, D.S.**, **Weigel, D.** ***et al.*** (2023) Spatial metatranscriptomics resolves host–bacteria–fungi interactomes. *Nature Biotechnology*, **42**, 1384–1393. Available from: https://doi.org/10.1038/s41587-023-01979-2

Schäfer, M., **Pacheco, A.R.**, **Künzler, R.**, **Bortfeld-Miller, M.**, **Field, C.M.**, **Vayena, E.** ***et al.*** (2023) Metabolic interaction models recapitulate leaf microbiota ecology. *Science*, **381**, eadf5121. Available from: https://doi.org/10.1126/science.adf5121

Schenk, R.U. & **Hildebrandt, A.C.** (1972) Medium and techniques for induction and growth of monocotyledonous and dicotyledonous plant cell cultures. *Canadian Journal of Botany*, **50**, 199–204. Available from: https://doi.org/10.1139/b72-026

Schlaeppi, K., **Dombrowski, N.**, **Oter, R.G.**, **Ver Van Loren, T.E.** & **Schulze-Lefert, P.** (2014) Quantitative divergence of the bacterial root microbiota in *Arabidopsis thaliana* relatives. *Proceedings. National Academy of Sciences. United States of America*, **111**, 585–592. Available from: https://doi.org/10.1073/pnas.1321597111

Sessitsch, A., **Pfaffenbichler, N.** & **Mitter, B.** (2019) Microbiome applications from lab to field: facing complexity. *Trends in Plant Science*, **24**, 194–198. Available from: https://doi.org/10.1016/j.tplants.2018.12.004

Shahan, R., **Hsu, C.-W.**, **Nolan, T.M.**, **Cole, B.J.**, **Taylor, I.W.**, **Greenstreet, L.** ***et al.*** (2022) A single-cell Arabidopsis root atlas reveals developmental trajectories in wild-type and cell identity mutants. *Developmental Cell*, **57**, 543–560.e9. Available from: https://doi.org/10.1016/j.devcel.2022.01.008

Shen, W., **Sipos, B.** & **Zhao, L.** (2024) SeqKit2: a Swiss army knife for sequence and alignment processing. *iMeta*, **3**, e191. Available from: https://doi.org/10.1002/imt2.191

Shulse, C.N., **Cole, B.J.**, **Ciobanu, D.**, **Lin, J.**, **Yoshinaga, Y.**, **Gouran, M.** ***et al.*** (2019) High-throughput single-cell transcriptome profiling of plant cell types. *Cell Reports*, **27**, 2241–2247.e4. Available from: https://doi.org/10.1016/j.celrep.2019.04.054

Siffert, A. & **Sasse, J.** (2024) Altered *Arabidopsis thaliana* sugar metabolism affects exudation, immune responses, and plant-microbe interactions. *bioRxiv*. Available from: https://doi.org/10.1101/2024.09.07.611788

Stuart, T., **Butler, A.**, **Hoffman, P.**, **Hafemeister, C.**, **Papalexi, E.**, **Mauck, W.M.** ***et al.*** (2019) Comprehensive integration of single-cell data. *Cell*, **177**, 1888–1902.e21. Available from: https://doi.org/10.1016/j.cell.2019.05.031

Tan, C., **Zhang, L.**, **Duan, X.**, **Chai, X.**, **Huang, R.**, **Kang, Y.** ***et al.*** (2022) Effects of exogenous sucrose and selenium on plant growth, quality, and sugar metabolism of pea sprouts. *Journal of the Science of Food and Agriculture*, **102**, 2855–2863. Available from: https://doi.org/10.1002/jsfa.11626

Torres, M., **Price, M.N.**, **Kashanova, A.**, **Kosina, S.M.**, **Zhalnina, K.**, **Northen, T.R.** ***et al.*** (2025) Bacterial fitness for plant colonization is influenced by plant growth substrate. *New Phytologist*, **248**, 3168–3190. Available from: https://doi.org/10.1101/2025.01.16.633496

Van Elsas, J.D., **Chiurazzi, M.**, **Mallon, C.A.**, **Elhottovā, D.**, **Krištůfek, V.** & **Salles, J.F.** (2012) Microbial diversity determines the invasion of soil by a bacterial pathogen. *Proceedings. National Academy of Sciences. United States of America*, **109**, 1159–1164. Available from: https://doi.org/10.1073/pnas.1109326109

van Gelderen, K., **Kang, C.** & **Pierik, R.** (2018) Light signaling, root development, and plasticity. *Plant Physiology*, **176**, 1049–1060. Available from: https://doi.org/10.1104/pp.17.01079

Walter, A., **Feil, R.** & **Schurr, U.** (2003) Expansion dynamics, metabolite composition and substance transfer of the primary root growth zone of *Zea mays* L. grown in different external nutrient availabilities. *Plant, Cell & Environment*, **26**, 1451–1466. Available from: https://doi.org/10.1046/j.0016-8025.2003.01068.x

Wippel, K., **Tao, K.**, **Niu, Y.**, **Zgadzaj, R.**, **Kiel, N.**, **Guan, R.** ***et al.*** (2021) Host preference and invasiveness of commensal bacteria in the lotus and Arabidopsis root microbiota. *Nature Microbiology*, **6**, 1150–1162. Available from: https://doi.org/10.1038/s41564-021-00941-9

Xiong, R., **He, X.**, **Gao, N.**, **Li, Q.**, **Qiu, Z.**, **Hou, Y.** ***et al.*** (2024) Soil pH amendment alters the abundance, diversity, and composition of microbial communities in two contrasting agricultural soils. *Microbiol Spectr*, **12**, e0416523. Available from: https://doi.org/10.1128/spectrum.04165-23

Yamada, K. & **Mine, A.** (2024) Sugar coordinates plant defense signaling. *Science Advances*, **10**, eadk4131. Available from: https://doi.org/10.1126/sciadv.adk4131

Yang, Z., **Zhang, L.**, **Diao, F.**, **Huang, M.** & **Wu, N.** (2004) Sucrose regulates elongation of carrot somatic embryo radicles as a signal molecule. *Plant Molecular Biology*, **54**, 441–459. Available from: https://doi.org/10.1023/B:PLAN.0000036375.40006.d3

Zhou, F., **Emonet, A.**, **Dénervaud Tendon, V.**, **Marhavy, P.**, **Wu, D.**, **Lahaye, T.** ***et al.*** (2020) Co-incidence of damage and microbial patterns controls localized immune responses in roots. *Cell*, **180**, 440–453.e18. Available from: https://doi.org/10.1016/j.cell.2020.01.013

Zhou, Y., **Liu, D.**, **Li, F.**, **Dong, Y.**, **Jin, Z.**, **Liao, Y.** ***et al.*** (2024) Superiority of native soil core microbiomes in supporting plant growth. *Nature Communications*, **15**, 6599. Available from: https://doi.org/10.1038/s41467-024-50685-3

Zhu, J., **Lolle, S.**, **Tang, A.**, **Guel, B.**, **Kvitko, B.**, **Cole, B.** ***et al.*** (2023) Single-cell profiling of Arabidopsis leaves to pseudomonas syringae infection. *Cell Reports*, **42**, 112676. Available from: https://doi.org/10.1016/j.celrep.2023.112676